An Analysis of Coexistence Curve Data for Several Binary Liquid Mixtures Near Their Critical Points

A. Stein and G. F. Allen

Department of Chemistry, Temple University, Philadelphia, Pa. 19122

Experimental data on the coexistence curves for nine binary liquid systems, which meet strict criteria of precision, purity of components, and experimental method, are analyzed in the neighborhood of the critical point. The data are examined in terms of a general equation of state which is nonanalytic at the critical point. The results of the computer analysis using weighted non-linear least squares procedures present evidence that some symmetry features of classical equations of state remain; and within the experimental errors in the data all systems are consistent with the critical exponent $\beta = 0.34$. The asymptotic behavior of the diameter is examined and evidence is provided for a curved diameter in some cases; however, it is concluded that the available data are not extensive enough to make a firm conclusion concerning the shape of the diameter. Experimental methods are briefly criticized and mention is made of the experimental direction that future work should take. Special attention is given to estimating the reliability of the conclusions that may be drawn from a given set of data.

Key words: Binary liquid mixtures, coexistence curve, consolute point, critically evaluated data, critical point, critical point exponent, diameter, power law, statistical analysis.

1. Introduction

Only a few years after Andrews [1][1] discovered the critical temperature of carbon dioxide, van der Waals [2] suggested that there is a continuity on passing from the gaseous to the liquid state. The famous van der Waals equation of state accounts qualitatively for vapor-liquid equilibrium and the existence of the critical point. This equation of state predicts that the coexistence curve is parabolic in shape. As pointed out in a recent publication by Levelt Sengers, Vincentini-Missoni, and Straub [3], there was by 1900 already evidence that the coexistence curve for a single component was more nearly cubic near the critical point. This cubic shape was in conflict with the classical theories of the day, such as the treatment of Van Laar [4] who postulated that the liquid and gas densities ρ^+ and ρ^-, respectively, can be written in terms of powers of the reduced temperature $\epsilon = (T - T_c)/T_c$ as

$$\rho^{\pm} = \rho_c(1 + B_1^{\pm}|\epsilon|^{\beta} + B_2^{\pm}|\epsilon|^{2\beta} + \ldots). \tag{1}$$

Using the assumption that the equation of state of a fluid is analytic at the critical point, and therefore may be expanded in a Taylor series in the density and temperature, van Laar showed that $B_1^+ = -B_1^-$, $B_2^+ = B_2^-$, and $\beta = 1/2$ or $1/4$. In recent years there has been an upsurge in interest in critical phenomena [5] and the discrepancy between theory and experiment has recently been resolved by acceptance of the idea that the free energy is nonanalytic in temperature and density at the critical point and a Taylor expansion of the equation of state of real fluids about the critical point therefore does not exist. This approach leads to an expression for the coexistence curve of the general form

$$\rho^{\pm} = \rho_c(1 + B_1^{\pm}|\epsilon|^{\beta_1^{\pm}} + B_2^{\pm}|\epsilon|^{\beta_2^{\pm}} + \ldots), \tag{2}$$

where ρ^+, ρ^-, are the liquid and gas densities, respectively, and $\beta_1^+ < \beta_2^+ < \ldots$, and $\beta_1^- < \beta_2^- \ldots$, hence the symmetry features of the classical case are lost.

However, Levelt Sengers and co-workers [3] in their careful analysis of highly precise data on the gas-liquid coexistence curves for several systems have found that $B_1^+ = -B_1^-$, $\beta_1^+ = \beta_1^-$, and very likely $B_2^+ = B_2^-$, $\beta_2^+ = \beta_2^-$. They furthermore demonstrated that the rectilinear diameter, $(\rho^+ + \rho^-)/2$, is a linear function of ϵ to within the error of experimental data. The present work deals with a similar study of the best existing data for the coexistence curves of binary liquid mixtures near their consolute points.

In 1945 Guggenheim [6] represented gas-liquid coexistence data by the equation

$$(\rho^+ - \rho^-) = k(T_c - T)^{1/3}. \tag{3}$$

This equation was applied to binary liquid systems by Zimm [7] and Rice [8] where they replaced ρ^+ and ρ^- by composition variables, either mole fraction or volume fraction for one of the components in each phase. In 1956 Cox and Herington [9] showed that the coexistence data could be represented over a larger range of temperature by the expressions:

$$(T - T_c)^{1/3} = A^+ \log \frac{X_1^+}{1 - X_1^+} + B^+, X_1 > X_{1c} \tag{4}$$

and

$$(T - T_c)^{1/3} = A^- \log \frac{X_1^-}{1 - X_1^-} + B^-, X_1 < X_{1c}, \tag{5}$$

where X_1^+ and X_1^- refer to the composition of the upper and lower phases, respectively and X_{1c} denotes the critical composition. In these equations $B^{\pm} = A^{\pm} \log$

[1] Numbers in brackets indicate literature references in section 7.

$\frac{1-X_c}{X_c}$ so that an expansion of the logarithm around X_c leads to the approximate form

$$X^{\pm}-X_c=K^{\pm}(T-T_c)^{1/3}, \tag{6}$$

and is therefore equivalent with equation (3) as modified by Rice and Zimm. In the neighborhood of the critical point the composition is, therefore, expected to be a linear function of $(T-T_c)^{1/3}$. A plot of $(X^{\pm}-X_c)$ versus $(T-T_c)^{1/3}$ has come to be known as a "Cox-Herington Plot".

In the mid-1950's Rice [10] suggested from theoretical consideration that the coexistence curves should in general be truncated (that is show a flat top) near T_c. This prediction stimulated considerable activity and most of the precise data available today are results of attempts to confirm or disprove the existence of this flat top. Usually the experimental data were analyzed using a modified Cox-Herington plot in which $X-X_c$ was plotted versus $|T-T_c+\delta|^{1/3}$ where δ is a small constant indicating the extent to which the curve is truncated. Rice and Thompson [11] in an extremely careful experiment showed in 1964 that to a temperature precision of ± 0.00005 °C and composition precision ± 0.003 percent no flat top existed for the system carbon tetrachloride–perfluoromethylcyclohexane. The Cox-Herington plot of their data is given in figure 1.[2]

Although in the past coexistence curve data for binary systems have often been represented by an exponent $\beta=1/3$ as justified by the linearity of a Cox-Herington plot this method is a very insensitive procedure for testing the correct value of the exponent. To illustrate this we have prepared Cox-Herington plots from the data of Thompson and Rice where $\beta=0.29$ and $\beta=0.38$ have been used instead of $\beta=0.33$ and T_c has been varied slightly to obtain the best fit. The results are shown in figures 2 and 3 showing that the experimental data appear to be equally well represented. Considering the fact that these data of Thompson and Rice are much more precise than any other existing data we conclude that it is not possible to decide between slightly different values of β by the Cox-Herington plots because of the inevitable scatter in the data. Indeed Rice and Thompson [11] recognized this difficulty when they replotted their data with an exponent $\beta=5/16$, the value calculated for the three dimensional Ising model, and concluded that 1/3 and 5/16 are not distinguishable from their data (at least by a Cox-Herington plot).

As mentioned in the review article by Heller [12] the exponent β has not generally been determined with the scaling ideas in mind for binary systems except in one or two cases. The scaling law equation for the coexistence curve is

$$\langle P\rangle \sim |\epsilon|^{\beta}, \tag{7}$$

where $\langle P\rangle$ represents an appropriate order parameter. One must keep in mind that eq (7) is taken to mean

$$\beta=\lim_{\epsilon\to 0}\frac{\log\langle P\rangle}{\log|\epsilon|}. \tag{8}$$

It is also of interest to examine the universality of the value of the coexistence curve exponent β for binary liquid systems. Whereas β had widely been supposed to be 1/3 for all types of critical systems, there exists a growing list of materials for which β has a significantly different value [13]. Furthermore, small deviations outside experimental uncertainties in the values of exponents which were thought to have universal values are now considered significant [13].

We here present a detailed computer analysis of the available high precision coexistence data for binary liquid systems. The data are analyzed from several different points of view and special attention is given to estimating the reliability of the conclusions which may be drawn from a given set of data. Experimental methods are briefly criticized and mention is made of the experimental direction that future work should take. It is shown that to within the experimental uncertainty of the data β is represented by a "universal" value. Also, evidence is presented that binary liquid coexistence curves are in general less symmetrical with respect to the critical composition X_c than those of gas-liquid systems, in the sense that

$$(X^{+}-X_c)\neq-(X^{-}-X_c), \tag{9}$$

in many cases, even close to T_c. It will be demonstrated that in spite of the condition of nonanalyticity at the critical point, which yields a coexistence curve equation

$$X_1^{\pm}=X_{1c}(1+B_1^{\pm}|\epsilon|^{\beta_1^{\pm}}+B_2^{\pm}|\epsilon|^{\beta_2^{\pm}}+\ldots) \tag{10}$$

where $\beta_1^{+}<\beta_2^{+}<\ldots$, $\beta_1^{-}<\beta_2^{-}<\ldots$, and $X_1^{\pm}$ represents the composition of component 1 in each phase, the results of this analysis can be consistent with $\beta_1^{+}=\beta_1^{-}$, $B_2^{+}\approx B_2^{-}$, $\beta_2^{+}=\beta_2^{-}$, and a third term on the right hand side in eq (10) which is relatively larger than in gas liquid systems. Furthermore, there is an indication, although the data are scant, that the diameter, $(X^{+}+X^{-})/2$, exhibits some degree of curvature close to T_c in several systems.

2. Experimental Data

2.1. Choice of Systems for Data Analysis

Much of the coexistence curve data in the older literature is not satisfactory for testing the power law ideas because the early workers did not concern themselves with careful temperature measurements and elaborate purification of the components which later appeared to be necessary. Since the power laws are only expected

[2] Figures and tables have been placed at the end of this paper.

to apply asymptotically in the region close to T_c the experimental data for a system to be analyzed must include a sufficient number of points near the extremum of the coexistence curve so that statistical methods can be applied; quite naturally many of the early studies on binary systems lack extensive data in this range. Some of the coexistence curve data in the literature are based on calculations assuming the law of the rectilinear diameter. Such data are not useful in an analysis such as ours since the validity of the law of the rectilinear diameter is questionable; it is examined in the latter part of this report.

In setting up our criteria for choosing systems from the literature to be analyzed, we had to compromise our desire to look at data of very high precision with the desire to examine more than just one or two systems. The four criteria we used, dictated largely by the availability of data in the literature are:

1. Temperature control and measurement must be at least to ± 0.01 °C.
2. The authors must demonstrate their concern for extensive purification and analysis of the components of the binary systems.
3. In the region close to $T_c(\epsilon = (T-T_c)/T_c < 10^{-3})$ there must be more data points than there are parameters in the power law equation *at the very least.*
4. There must be no assumptions, such as the rectilinear diameter law, which would bias the results of the data analysis.

The systems chosen for data analysis in this report are indicated in section 2.2.[3]

No attempt is made to include an exhaustive bibliography of all the experimental determinations of the coexistence curves for binary systems since these are included in a recent comprehensive bibliography by Michaels, Green, and Larsen [15].

2.2. The Individual Systems Chosen for Data Analysis

In table I the various systems are listed approximately in order of descending precision and overall reliability of the work. We here discuss each system briefly in the same order.

A. Perfluoromethylcyclohexane–carbon tetrachloride studied by Thompson and Rice [11] (1964), provides the most precise determination of a coexistence curve to date. The relative temperatures in this study were measured by a very sensitive liquid-in-glass thermometer (diethyl phthalate in Pyrex) of special design to a precision of $\pm 5 \times 10^{-5}$ °C ($\epsilon \approx 2 \times 10^{-7}$). The densities of the upper phases were measured in a closed double thermostated system by a mechanical quartz-helix densitometer to a precision of ± 0.003 percent. The densities for the corresponding bottom phases were then calculated from the over-all density of the sample, D_s; the density of the top phase, D_t; the length of the sample, L; and the length of the bottom phase, l_b according to the equation

$$D_b = (D_s - D_t)L/l_b + D_t. \tag{11}$$

The lengths L, l_b in the above equation were determined from the meniscus positions and were corrected to what they would be if the sample were in the shape of a cylinder. Corrections were also applied to account for density gradients due to gravity for each phase and a larger density gradient in the lower phase attributed to less effective mixing in the lower regions of the sample. It is stated that changes in density will be proportional to changes in composition over a small range of temperature (which was 0.006 °C corresponding to 0.2 percent change in density). The critical temperature could not be determined directly to the precision of the temperature measurements; rather it was estimated as the value which produced the best straight line when density was plotted versus $(T-T_c)^{1/3}$.

B. 3-Methylpentane–nitroethane was studied by Wims, McIntyre, and Hynne [16] (1968) by means of an ingenious magnetic densitometer. They were able to measure the densities of both coexisting phases in a closed system by measuring the current in a solenoid coil necessary to suspend a magnetic float of known density in the liquid. It is stated that a plot of density versus volume fraction (volumes before mixing) was linear, which indicates that any volume change upon mixing of the components is small since density, ρ, and volume fraction (before mixing), ϕ_1, are related by

$$\rho = (\rho_1 - \rho_2)\phi_1 + \rho_2, \tag{12}$$

where ρ_1 and ρ_2 are the densities of the pure components. Volume fractions were calculated from eq (12) and then converted to mole fraction. All three variables are used to represent the data.

Had these workers been able to control the temperature to ± 0.0001 °C, rather than ± 0.001 °C, their results would have equalled and in some ways surpassed the results of Thompson and Rice [11]. Densities in this work were precise to ± 0.027 percent. It is interesting to note that Wim's report on this system is the first example of careful data analysis of coexistence curve data, the results of which are in excellent agreement with the present report.

C. Cyclohexane–diiodomethane was studied by Irani and Rice [17] (1967) using visual observation of the appearance of the meniscus as highly purified, sealed binary mixtures were cooled in the one phase region. Temperatures in this study were controlled and measured to ± 0.001 °C. Compositions were determined by

[3] A few systems studied by O. K. Rice and his students, most notably cyclohexane-aniline [29] which apparently meet our criteria for analysis were not analyzed. In these cases the data near T_c are sufficiently scattered that data analysis is impossible and it is this scatter which apparently led Rice to the conclusion that the coexistence curve was truncated.

weighing the pure components before preparing solutions and were precise to ±0.21 percent. The composition variable is mole fraction.

D. Loven and Rice [18] (1963) studied the system 2,6-dimethylpyridine–water which has a lower consolute temperature. They used visual observation of the meniscus appearance, and controlled and measured temperatures to ±0.001 °C. Their solutions were prepared on a volume basis (volumes before mixing) with a precision of about ±0.66 percent. The volume fractions were then converted to mole fractions and both composition variables are reported.

E. Triethylamine–water also having a lower consolute temperature was studied by Kohler and Rice [19] (1956) by visual observation of the appearance of the meniscus. The compositions of the solutions were determined by titration which yields mole fraction. The mole fractions were converted to volume fractions and both variables are reported. While temperatures were controlled and measured to ± 0.001 °C the value of the critical temperature is reported only to ± 0.01 °C. The mole fractions are reported precise to ±0.12 percent and volume fractions to ±0.75 percent. Due to the basic nature of triethylamine it is likely that these mixtures contained small amounts of impurities produced by reactions with the glass containers.

F. Kao and Chu [20] (1968) reported a determination of the coexistence curve of *n*-decane-β,β'-dichlorodiethylether by visual observation of the appearance of the meniscus of various mixtures prepared by weight. While their temperatures are reported to ± 0.001 °C, they were plagued with inconsistent critical temperatures possibly due to decomposition or impurities. The composition variable is mole fraction and is reported to be precise to about ± 0.1 percent.

G. Isobutyric acid – water was reported on by Woermann and Sarholz [21] (1965) who used the visual method to determine the separation temperatures on samples prepared by weighing and mixing the pure components. They reported their temperatures to a precision of ± 0.01 °C and mole fractions to ± 0.8 percent.

H. The water – ethylene glycol monoisobutyl ether system was examined by Rudd and Widom [22] (1960) with temperatures reported to ± 0.01 °C. They used the visual method of observation of the meniscus appearance on solutions prepared by weight. Mole fractions are reported to ± 0.8 percent. There are not many data points close to T_c, and the authors suggest that there may be impurities in large enough amounts to affect their results.

I. Methyldiethylamine – water as reported by Copp [23] (1955) represents the oldest data that were chosen for analysis. Again the visual method was used on samples prepared by weight. Mole fractions were converted to volume fractions (before mixing), and are reported precise to only ± 6 percent. Temperatures were reported to ± 0.01 °C.

3. Method of Analysis

3.1. Statistical Procedures and Curve Fitting

The coexistence curve data, that is, separation temperatures and compositions were analyzed by the non-linear least squares curve fitting methods of Deming [24] in conjunction with a grid searching method. In Deming's procedure both experimental variables associated with a datum point (in our case temperature and composition) are considered subject to error. For every experimental point a corresponding point is calculated on the least squares curve giving rise to an "adjusted point." The degree to which each coordinate of a point is adjusted is proportional to the weight given to that coordinate. The relative weight assigned each coordinate is determined from the experimental uncertainty in measuring the corresponding property. The function to be fitted is written as

$$F_i(T_i, X_i, A, \beta \ldots) = 0, \tag{13}$$

where $A, \beta \ldots$ are parameters of the equation to be determined by the least squares procedure. Equations (13) are linearized by a Taylor expansion around the experimental variables and approximate parameters in which any terms higher than first order are discarded. The parameters of the fit are calculated by analytically solving the normal equations for the parameter residuals. This procedure is in contrast to some popular methods in which the least squares sum is minimized by iterative procedures. In Deming's method the weighting function associated with the normal equations is defined by

$$\frac{1}{W_{F_i}} = \left(\frac{\partial F}{\partial T_i}\right)^2 \sigma_{T_i}^2 + \left(\frac{\partial F}{\partial X_i}\right)^2 \sigma_{X_i}^2, \tag{14}$$

where σ_{T_i} is the reported precision in the temperature and σ_{X_i} is the reported precision in the composition for the ith data point. In addition to the Deming procedure it is sometimes convenient to simply vary one or two parameters of the equation in a systematic fashion, while calculating the remaining parameters at the same time until the best fit is obtained. The least squares sum or chi-square is calculated for all values of parameters which are being incremented, and the resulting χ^2 surface (χ^2 as a function of the parameters which are varied) is examined for the minimum. Since the weighting function usually contains several parameters, care is taken to ensure an accurate determination of the chi-square surface by iterating with the optimum values of all parameters upon each step of the process. This procedure constitutes the grid search. One advantage of the grid searching procedure is that additional insight about the behavior of the function being fitted sometimes results from examination of the χ^2 surface. A second advantage is that parameters which must be restricted only to values that are physically significant

are easily accommodated by this procedure.

In the course of this analysis it was found that the values of the calculated parameters usually depended strongly on the value assumed for T_c. Since often the value of T_c is not known as precisely as the other separation temperatures along the coexistence curve the dependence of the parameters on T_c leads to considerable difficulty in fitting the data. It might at first appear that the way around this difficulty is to treat T_c as a variable parameter to be optimized during the least squares procedure. This is not an entirely satisfactory solution, however, since there is a tendency for the optimized value of T_c to lie unrealistically close to the nearest experimental separation temperature when in fact we know that T_c should correspond to the maximum in the coexistence curve. This problem comes about because the points close to the top of the curve have small weights (since ΔT is small) as compared to the points farther away. χ^2 appears to be lowered by optimizing T_c as close as possible to the nearest experimental point and readjusting the fitted parameters accordingly because the values of the weights, on which χ^2 depends, are lowered accordingly. To avoid this difficulty T_c is considered as an experimental value (which of course it is) to which we can assign an approximate weight estimated from the error in determining T_c. This leads us to a modified definition of χ^2 as

$$\chi^2 = \sum_{i=1}^{N} \left\{ \left(\frac{XRes_i}{\sigma_{X_i}} \right)^2 + \left(\frac{TRes_i}{\sigma_{T_i}} \right)^2 \right\} + \left(\frac{(T_c^{exp} - T_c)}{\sigma_{T_c}} \right)^2, \quad (15)$$

where T_c^{exp} is the experimental value reported by the investigator, T_c is the optimized value and σ_{T_c} is the estimated experimental error associated with T_c^{exp}. *TRes* and *XRes* represent the experimental minus the calculated values for temperature and composition, respectively. σ_{T_i} and σ_{X_i} are the experimental errors in T and X. Thus, by defining χ^2 in this manner it can be minimized while treating T_c as well as T and X as experimental parameters subject to error during the adjustment procedure in accordance with statistical methods.

The quality of the fit of the experimental data to the model equation is determined by the magnitude of the reduced chi-square, which is defined as

$$R\chi^2 = \frac{\chi^2}{N - P}, \quad (16)$$

where N is the number of experimental points, P is the number of parameters in the model equation, and χ^2 is defined by eq (15). For any set of experimental points of known precision, which obey a known functional relationship, the probability that the reduced chi-square has a value of 1.0 or greater due to random fluctuations is approximately 50 percent, and in the limit as the number of points becomes infinite the reduced chi-square equals unity. This probabilistic interpretation of the reduced chi-square, of course, is valid only if the errors in the data are random and the equation used in the fitting procedure is the correct one. High values of the reduced chi-square and random deviations of the experimental points from the calculated curve indicate that the reported precision of the data is too high. Similarly, if the reduced chi-square is much less than unity, the reported precision of the data is probably too conservative. However, high values of $R\chi^2$ and systematic deviations of the experimental points from the calculated curve indicate that the model equation used to fit the data is not a good representation of the data, and, therefore, very little confidence should be placed in the values of the calculated parameters. Also, it should be mentioned that when the number of experimental points approaches the number of parameters to be determined, the χ^2 probability distribution becomes very broad and the χ^2 surface very complex so that it is rather difficult to find true optimum values for the parameters.

The standard deviations, σ, of least squares calculated parameters may be estimated from the diagonal elements of the variance-covariance matrix, which is obtained by inverting the matrix of the coefficients of the parameter residuals in the normal equations. If the data are weighted using absolute weights (the reciprocals of the variances), the reduced chi-square, defined by eq (16), should be approximately 1.0, and the square roots of the diagonal elements of the variance-covariance matrix are the parameter deviations, according to Deming's statistical formulation [24]. In cases where the reduced chi-square is greater than unity, which usually indicates that the data is not as precise as it was originally thought to be, one usually revises the estimate of precision such that $R\chi^2 \approx 1.0$ and refits the data. However, since this report concerns data from the literature and one of the objectives of this analysis is to assess the accuracy of the data, the values of the reduced chi-square's obtained with the reported values of precision are of interest. Therefore, the following procedure is used.

When the reduced chi-square is greater than unity, the square roots of the diagonal elements of the variance-covariance matrix are multiplied by the square root of the reduced chi-square to yield the parameter deviations. This procedure for calculating parameter deviations is effectively independent of the reported values of the precision of the data, and in fact, is probably the most common method for obtaining parameter deviations. When the reduced chi-square is less than unity, indicating a possibly conservative estimate of the precision of the data, the parameter deviations are taken simply as the square roots of the diagonal elements of the variance-covariance matrix. Thus, if the reported precision is too high, the reduced chi-square will be high, but the parameter deviations will not be influenced. If the reduced chi-square is less than 1.0,

due either to conservatively reported precision or by chance (which is quite possible with a small number of data points), the parameter deviations will either be conservative or "correct", respectively.

The method of obtaining parameter deviations described above has one further advantage. It was necessary in this analysis to calculate values for parameters from data which had been partially "smoothed" in order to use two of the model equations which were desired. As a consequence of this "smoothing procedure" a small amount of the "scatter" in the data was removed. Therefore, erroneous standard deviations for the parameters (parameter deviations would be too small) would result, if the parameter deviations were calculated from the scatter in the data, which is the usual procedure, as mentioned above. Deming's method, however, should yield approximately correct parameter standard deviations in these cases.

Computations and curve fittings were carried out by means of programs written in Fortran for the Temple University CDC 6400 Computer.

3.2. Obtaining the Exponent β

The model equation used for the description of the coexistence curve for a binary system is

$$< P >= A\,|\epsilon|^{\beta}, \tag{17}$$

where $\epsilon = \dfrac{|T - T_c|}{T_c}$, $<P>$ represents an appropriate order parameter representing the composition variable. For convenience we have fitted the various sets of data using the logarithmic form of eq (17):

$$ln < P >= \beta\, ln\, \epsilon + ln\, A. \tag{18}$$

It is apparent that experimental uncertainties (or "scatter") in the data, which usually become quite noticeable near T_c, must cause the optimized parameters to depend slightly on the statistical weights assigned to each experimental point. The weighting function consists of one term depending on the precision to which the composition is determined and another term, which greatly increases near T_c reflecting the "propogated error" due to uncertainties in the measurement of temperature. For example, the weighting function for eq (18) is

$$\frac{1}{W_{F_i}} = \left(\frac{\beta}{T_c \epsilon}\right)^2 \sigma_{T_i}^2 + \left(\frac{1}{< P >_i}\right)^2 \sigma^2_{< P >_i} \tag{19}$$

where W_{F_i} is the weight, $\sigma^2_{T_i}$ the variance of the temperature, and $\sigma^2_{\langle P\rangle_i}$ the variance of the order parameter for the ith point. The first term accommodating the experimental error in the temperature has the effect of decreasing the weights of the data points near T_c. As can be seen from eq (18), the logarithmic form of eq (17) makes the weight decrease even more pronounced. The ϵ range for which the propogated error dominates the weighting function depends on the precision of the composition variable (order parameter). However, the power law equation is valid only asymptoically near T_c while the values of the parameters determined by the least-squares procedure are more heavily influenced by the data away from T_c. J. M. H. Levelt Sengers and co-workers [3] have discussed this problem in connection with their very careful analysis of data for several gas-liquid coexistence curves. For these one-component systems there are usually enough experimental data points so that the quality of the fit to the power law equation can be examined as a function of the number of points used in the fitting procedure. The least-squares procedure is repeated successively with fewer and fewer points, leaving out those data points farthest from T_c, until the quality of the fit (χ^2) becomes essentially constant and deviations appear to be random. The temperature at which this constancy occurs is taken to define the asymptotic region in which the power law is valid. Unfortunately, it is not possible to apply this range-narrowing technique to most of the experimental results available for binary systems because the number of data points is very small. If the range-narrowing procedure were applied the number of points available for the curve fitting procedure would approach the number of parameters to be determined and therefore confidence in the calculated parameters would be greatly decreased.

The choice of the order parameter to be used in analyzing coexistence curve data is by no means trivial. Ideally one would prefer to have temperature composition data at the extremes of the tie-line connecting the two sides of the coexistence curve. That is, for every separation temperature it is desirable to know the composition of both coexisting phases in which case the order parameter would be $|X^+ - X^-|$ where X^+ represents the composition of the upper phase and X^- that of the lower phase. Unfortunately, most of the experimental data available to us were obtained by noting the temperature at which the meniscus separating the two phases appeared. Many samples of known composition are prepared and cooled from the one phase region until the meniscus becomes apparent by visual observation. This way the two sides of the coexistence curve are determined separately and compositions of the upper and lower phases corresponding to the same separation temperature are not obtained.

One expedient choice for an order parameter which satisfies the theoretical requirements is $|X - X_c|$, where X_c represents the critical composition for the system. The data for all systems listed in table I were fit to the power law expression:

$$|X-X_c| = A\,|T-T_c|^{\beta}, \tag{20}$$

where X_c and T_c were optimized by a grid searching procedure with the equation written in logarithmic form

$$\ln|X-X_c| = \beta \ln|T-T_c| + \ln A. \tag{21}$$

The parameters A and β were calculated upon each iteration of the grid searching procedure by the method of Deming.

It has been repeatedly stated in the literature that the composition for each side of the coexistence curve is a linear function of $|T-T_c|^{1/3}$. With this in mind we represent each branch of the coexistence curve by a separate power law equation

$$(X^+-X_c) = A^+|T-T_c|^{\beta^+} \text{ for } X^+ > X_c, \tag{22a}$$

and

$$(X_c-X^-) = A^-|T-T_c|^{\beta^-} \text{ for } X_c > X^-, \tag{22b}$$

where the superscripts + and − refer respectively to the right and left sides of the coexistence curve. It should be noted that eqs (22) differ from the Cox-Herington equations where $\beta^+ = \beta^- = 1/3$. The coexistence data were fitted to eqs (22) with the restriction that X_c and T_c must be the same for each side of the curve. This was accomplished by minimizing

$$\chi^2 \text{ Total} = (\chi^2)^+ + (\chi^2)^-, \tag{23}$$

with respect to the parameters A^+, A^-, β^+, β^-, and X_c. T_c was taken as a weighted experimental value as described above. $A^{\pm}$ and $\beta^{\pm}$ were calculated by Deming's procedure upon each iteration of X_c and T_c.

A third method of representing the coexistence curve is based on suggestions made by Rice [8] and Zimm [7] in which the model equation,

$$X^+ - X^- = A|\epsilon|^{\beta}, X^+ > X^- \tag{24}$$

where X^+ refers to the composition of one phase and X^- to the coexisting phase, is used for the curve fitting procedure. The direct application of this equation to the experimental data requires that for each temperature below the critical temperature for which the composition of one phase is measured the composition of the coexisting phase is also determined. Only two systems included in this analysis were studied in this manner, C_7F_{14}—CCl_4 by Rice and Thompson [11] and nitroethane-3-methylpentane by Wims and coworkers [16].

For the remaining systems the application of eq (24) requires a different technique since for a given separation temperature only one composition is known. It was found that coexistence data may be represented very well by equations of the type

$$X^+ = A^+ + B^+|T-C^+|^{d^+} \tag{25a}$$

$$X^- = A^- + B^-|T-C^-|^{d^-} \tag{25b}$$

where the parameters $A^{\pm}$, $B^{\pm}$, $C^{\pm}$, $d^{\pm}$ are all optimized. These equations should be regarded simply as empirical interpolation functions for obtaining a value for the composition at a temperature where the experimental composition had not been measured. No physical significance should be given to the parameters in eqs (25). Equations (25) represent the data so well that practically all experimental points, (X, T) on one side of the coexistence curve may be calculated to within the experimental precision from a set of parameters, A, B, C, d corresponding to that side of the curve. The deviation plots for the Thompson-Rice data [11] fitted to eqs (25a) and (25b) are displayed in figure 13. The order parameter X^+-X^- was then obtained in the following manner. For every experimental composition X^+ for which the corresponding value X^- had not been measured, a value of X^- was calculated from eq (25b) using the parameters optimized for that side. Likewise for each experimental value of X^- for which there was no measured value of X^+, X^+ was calculated from eq (25a). This order parameter consisting of one experimental point and one point from the smooth curve was then used in fitting the entire curve to the equation

$$X^+ - X^- = A|\epsilon|^{\beta}. \tag{26}$$

While this method is not completely satisfactory from a statistical point of view, it is much better than calculating the order parameter (X^+-X^-) from both smoothed branch curves. By using a calculated point with an actual experimental point we have preserved some of the randomness in the data. The calculated points were weighted as if they were experimental points, which is a good approximation since the error of a calculated point is always less than that of an experimental point and the quantity of interest is, for instance $(X^+-X^-_{(\text{calc.})})$.

Fortunately, the data of Thompson [11] and Wims [16] allowed a check on this procedure. We fit the coexistence curves for these systems both using the experimental values of (X^+-X^-) directly in eq (24) and by smoothing each side of the curve, using an experimental point with a smoothed composition. The agreement both in the optimized parameters and in the values of the reduced χ^2 were excellent.

Whenever sufficient information was given by the experiments several different composition variables (mole fraction, volume fraction, density) were used as order parameter. Unfortunately, we could not analyze all the systems using the same order parameter for comparison.

3.3. Fitting the Diameter

The "diameter" defined as $\bar{X}=(X^+ + X^-)/2$ was also fitted to a power law equation

$$\bar{X}/X_c = 1 + a\epsilon^p. \tag{27}$$

The method of curve fitting was to grid search the parameter p while calculating the parameters a and X_c from Deming's procedure at the same time. T_c was taken as the optimized value from the coexistence curve analysis. Necessarily, $\bar{X}$ was obtained from an experimental plus a calculated value for most of the systems where the corresponding compositions at a given temperature were not measured as in the coexistence curve analysis. It must be emphasized that the sensitive quantity, $\bar{X}$, if obtained from a totally "smoothed" coexistence curve would be very unreliable and misleading.

Weighting was accomplished as follows:

$$F = \bar{X} - X_c - aX_c\epsilon^p. \tag{28}$$

and the weighting function is

$$\frac{1}{W_F} = \left(\frac{\partial F}{\partial \bar{X}}\right)^2 \sigma_{\bar{X}}^2 + \left(\frac{\partial F}{\partial T}\right)^2 \sigma_T^2, \tag{29}$$

$$= \sigma_{\bar{X}}^2 + \left(\frac{aX_c\epsilon^{p-1}}{T_c}\right)^2 \sigma_T^2, \tag{30}$$

where

$$\sigma_{\bar{X}}^2 = \frac{1}{4}\left[\sigma_{X^+}^2(T) + \sigma_{X^-}^2(T)\right]. \tag{31}$$

The variance $\sigma_{X^+}^2(T)$ and $\sigma_{X^-}^2(T)$ are functions of temperature and increase near T_c, while the second term on the right hand side in eq (29) is small for $p \approx 1$. Using the parameters β and A from the previous fit the whole weighting function to a good approximation is

$$\frac{1}{W_F} \approx \frac{1}{4}(\sigma_{X^+}^2 + \sigma_{X^-}^2) + \left(\frac{\beta A\epsilon^{\beta-1}}{2T_c}\right)^2 \sigma_T^2 + \left(\frac{aX_c\epsilon^{p-1}}{T_c}\right)^2 \sigma_T^2. \tag{32}$$

While the experimental error in the quantity $(X^+ - X^-)$ is of the same order of magnitude as the error in the quantity $|\bar{X} - X_c|$, the later quantity is obviously much smaller, going to zero for all values of ϵ for a perfectly symmetrical coexistence curve. This fact manifests itself in the precision to which it is possible to obtain the parameters a and p.

4. Results

4.1. Coexistence Data Fitted to $|X - X_c| = A|T - T_c|^\beta$

In view of eq (10) coexistence data would not be expected to fit this equation well unless, (a) the second and higher terms of eq (10) are small enough to be neglected, (b) $B_1^+ = -B_1^-$, and (c) $\beta_1^+ = \beta_1^-$. The results of this fitting procedure are presented in table II, and the deviation plots for the various systems are given in figures 4 to 12. The parameter β deviates significantly from the value of 1/3 for several systems. Also, the deviation plots clearly indicate that the coexistence curve is not symmetrical about X_c for some systems, and therefore, the choice of $|X - X_c|$ as the order parameter is, in general, inappropriate.

4.2. Coexistence Data Fitted to

$$(X^+ - X_c) = A^+|T - T_c|^{\beta+},\ X^+ > X_c,$$

$$(X_c - X^+) = A^-|T - T_c|^{\beta-},\ X_c > X^-$$

The coexistence data would not be expected to fit well to these equations unless the second and higher terms of eq (10) are small relative to the first term. Differences between A^+ and A^-, β^+ and β^- can obviously be accomodated by the equations. The results of this fitting procedure are shown in table III. The general trend is that the reduced chi-square values are lower than for the fit in which $|X - X_c|$ is taken as the order parameter for the whole coexistence curve according to eq (20). Table III shows that β and A differ, in general, for each side of the curve, β again significantly differing from 1/3 in many cases. The systematic deviation plots (which have not been included in the report) and the reduced chi-square values, which will be shown to be higher than those of the following fit, indicate that the data do not, in general, fit well to these equations.

4.3. Coexistence Data Fitted to $X^+ - X^- = A|\epsilon|^\beta$, where $X^+ > X^-$

The coexistence data would not be expected to fit well to this equation unless $\beta_1^+ = \beta_2^-$ and the higher order terms in eq (10) approximately cancel upon forming the quantity $X^+ - X^-$ or are small. The results of this fitting procedure are shown in table IV. The values of the reduced chi-square's are lower than those of all previous fits, and the deviation plots indicate that the data fits the equation rather well, as shown in figures 14 through 26.

Naturally, one would like to compare the data from all of the systems at the same time. To this end we have fitted all the data to the equation

$$\log(X^+ - X^-) - \log A = \beta \log|\epsilon|, \tag{33}$$

using the least squares values of A and T_c for each system in table IV. Figure 27 displays the results of this calculation where it should be noted that the composition variables used to form the order parameter are not

the same for all systems. The calculated least-squares parameter β from the fit to eq (33) is $\beta = 0.342 \pm 0.016$ and the reduced chi square is 22.6. (The error in A was considered upon assigning weights.)

Within our carefully estimated parameter deviations it appears that β for all systems listed in table IV lies between 0.33 and 0.35 when the order parameter is taken as $X^+ - X^-$.

4.4. The Diameter

Levelt Sengers, et al. [3] have recently reported that for several high precision gas-liquid systems the diameter defined as $\bar{X} = (\rho^+ + \rho^-)/2$ where ρ^+ and ρ^- are the liquid and vapor phase densities, is a linear function of the reduced temperature within experimental errors. They also conclude that if a curved diameter of the form $\bar{X} \sim |\epsilon|^{1-\alpha}$ is admitted where α is the static scaling law exponent for the specific heat, as was recently suggested in some model calculations [25–27] and also on thermodynamic grounds [28], a slightly negative value of α is favored contrary to the general consensus that α is probably positive and perhaps as large as 1/8. The present data for binary liquid systems, however, suggest that in some systems the diameter is curved for small values of ϵ (less than 10^{-3}).

The diameter, $\bar{X} = (X^+ + X^-)/2$ would be expected to obey a simple power law (asymptotically at least) if $B_1^+ = -B_1^-$, $\beta_1^+ = \beta_1^-$, and $\beta_2^+ = \beta_2^-$ in eq (10). In this case the first terms in eq (10) cancel, and $p = \beta_2^+ = \beta_2^-$ in the equation,

$$\bar{X}/X_c = 1 + a\epsilon^p. \tag{34}$$

The results of fitting the diameter to eq (34) are presented in table V. The values for the exponents (p) describing the curvature of the diameters are shown to vary generally from about 0.6 to 1.0 depending upon the particular system studied and to a smaller extent the composition variable used in the fitting procedure. Plots of the diameter versus ϵ are displayed in figure 28 through 40 where the fitted curve has been drawn in. Deviation plots for these fits are shown in figures 41–53.

5. Discussion and Conclusions

Coexistence data obtained by methods which measure the compositions of both coexisting phases as a function of temperature are particularly useful for studying the asymptotic behavior of the coexistence curve, and essential for accurately determining the asymptotic behavior of the diameter. As mentioned above, only two systems included in this analysis were studied in this manner, C_7F_{14}–CCl_4 by Rice and Thompson [11] and nitroethane–3-methylpentene by Wims and co-workers [16]. In both cases the composition variable measured was the density of each phase. Rice and Thompson [11] measured the density of only one phase by observing the length of a quartz helix to which was attached a float of known density. They calculated the density of the coexisting phase as described in section 2. Wims, et al. [16] using the magnetic densitometer described in section 2, was able to determine directly the density of both phases. A distinct advantage of these methods, apart from the data analysis, is that the entire coexistence curve can be determined from one sealed sample of critical composition, thereby eliminating the experimental uncertainty in preparing the several solutions needed for the visual observation of the appearance of the meniscus.

For the remaining systems the quantities $(X^+ \pm X^-)$ had to be obtained from partially "smoothed" data. Since a "smoothed point" always corresponds to an experimental point, a good deal of randomness in the data is still maintained, and any systematic errors imparted to the data should be quite minimal. However, in fitting the diameter the quantity of interest is really $|\bar{X} - X_c|$ which goes to zero for coexistence curves which are symmetrical with respect to X_c. Therefore, errors in $\bar{X}$ are more serious, and the exponents obtained for the behavior of the diameter for these systems should not be taken too seriously, but merely as an indication of the most probable behavior of the diameter near T_c.

Unfortunately, this data analysis suggests that the high precision Thompson-Rice [11] data contain some systematic experimental errors, probably arising from the magnitude of a correction factor which was applied for density gradients in the lower phase. The extremely curved diameter for their data is most probably a consequence of this experimental systematic error. Their data provide an example of how errors, which are relatively not serious in determining β can be quite serious in determining p for the diameter. Thus, the best evidence for a curved diameter is the data on nitroethane-3-methylpentane by Wims and co-workers [16], and to a lesser extent, the results for some of the other systems, which should be regarded in a more qualitative sense.

Several conclusions can be made concerning the asymptotic behavior of the coexistence curve near T_c. The data were analyzed in terms of an equation representative of nonanalyticity at the critical point,

$$X_1^{\pm} = X_{1_c}(1 + B_1^{\pm}|\epsilon|^{\beta_1^{\pm}} + B_2^{\pm}|\epsilon|^{\beta_2^{\pm}} + \ldots) \tag{10}$$

where $\beta_1^+ < \beta_2^+ < \ldots, \beta_1^- < \beta_2^- < \ldots$. Levelt Sengers, Straub, and Vincentini-Missoni [3] have pointed out that a near cancellation of higher order terms in eq (10) occurs upon taking the difference $\rho^+ - \rho^-$ in the case of gas-liquid systems. They concluded that in spite of the nonanalyticity, certain symmetry features established by van Laar [4] for the classical case seem to be present in real gases as well, namely, $B_1^+ = -B_1^-$, $\beta_1^+ = \beta_1^-$, and very likely $B_2^+ \approx B_2^-$, $\beta_2^+ = \beta_2^-$. All of the results of this data analysis for binary liquid mixtures can be represented by eq (10) if $\beta_1^+ = \beta_1^- = \beta$, where β

lies between 0.33 and 0.35; $B_2^+ \approx B_2^-$, $\beta_2^+ = \beta_2^-$. Upon forming the difference $X^+ - X^-$, the data fit well to a simple power law equation. It appears that the higher order terms in eq (10) cancel, and the simple power law behavior implies that $\beta_1^+ = \beta_1^-$. The presence of a rather large second term in eq (10) can explain why the data do not fit well to the equations in which the order parameters are $|X - X_c|$ and $X^\pm - X_c$. It was not possible to determine whether $B_1^+ = -B_1^-$ since a range narrowing analysis could not be done due to the paucity of data points. However, the asymptotic symmetry $B_1^+ = -B_1^-$ is certainly plausible.

The present existing data are still rather inconclusive with respect to the finer details of the asymptotic behavior of the coexistence curve for binary liquid systems. Data where both compositions are measured at each temperature are needed. Evidence has been presented that the critical point exponent for the coexistence curve β is very close to 1/3 for binary liquid systems and is, therefore, essentially the same as in gas-liquid systems [3]. Although the data are not extensive enough to study the effects of different composition variables on the shape of the coexistence curve, the coexistence curve for binary liquid systems appears to be more symmetrical with respect to the critical composition when compositions are expressed in volume fraction (volumes before mixing) rather than mole fraction. Also, no apparent correlation exists between the direction to which the diameter curves (high or low density side) and the type of chemical system or type of critical mixing point (upper or lower). A precision in temperature of ± 0.001 °C and about ± 0.17 percent in composition is sufficient in order to determine β precisely. However, it appears that greater precision is necessary to determine the asymptotic behavior of the diameter. The Thompson Rice [11] precision of ± 0.003 percent in density and $\pm 5 \times 10^{-5}$ °C in temperature would be desirable if the densities of *both* phases are measured.

6. Comments

A. Perfluoromethylcyclohexane–Carbon Tetrachloride [11]

In spite of excellent choice of the experimental method, the high precision in determining the densities and temperatures of the upper phase, and the great care used to insure that the components were of high purity the entire coexistence curve is probably not determined to the degree of accuracy which might be expected. As mentioned above, the densities of the lower phases were calculated, and a correction was applied for density gradients. The uncertainty in these calculations may account for the strong curvature of the diameter, $p < \beta$, which is highly unlikely. Since only relative temperatures were reported by the authors we have arbitrarily taken the highest reported value as 28.62600 in this report.

B. Nitroethane–3-Methylpentane [16]

Only densities were measured directly; the mole fractions and volume fractions were calculated by Wims, et al. [16] assuming no volume change upon mixing the components, and are therefore less reliable. The coexistence curve is slightly unsymmetrical with respect to the critical density as can be seen from the deviation plot, figure 5, for the fit $|X - X_c| = A|T - T_c|^\beta$. The diameter possesses a slight but distinct curvature for $\epsilon < 10^{-3}$ as shown in figures 29 to 31. Since the densities of the coexisting phases were measured directly at a series of temperatures, this work must be taken as the most reliable measurement of the coexistence curve and diameter to date. Unfortunately, even in this work, there are not enough data points close to T_c to accurately determine the behavior of the diameter.

C. Cyclohexane–Diiodomethane [17]

The coexistence curve is quite symmetrical with respect to the critical composition as can be seen from the deviation plot, figure 6 for the fit $|X - X_c| = A|T - T_c|^\beta$ and from the comparison of the β's obtained for different methods of fitting the coexistence data, tables II, III, and IV. The fact that $\bar{X} \approx X_c$ accounts for the large deviation for the exponent p which describes the diameter. For this system the diameter is best represented by a straight line. Since $|\bar{X} - X_c|$ is very small it is difficult to make a firm conclusion about the behavior of the diameter in this case.

D. 2,6-Dimethylpyridine–Water [18]

The coexistence curve for this system appears to be more symmetrical when the composition is expressed in volume fraction (volumes before mixing) rather than mole fraction. As can be seen from table IV, β is insensitive to the choice of composition variable while the diameter shows more curvature when mole fraction rather than volume fraction is taken as the composition variable. This behavior can be seen in table V and figures 33 and 34. Since $\bar{X} \approx X_c$ when the composition is expressed in volume fraction and the temperature range for the study is small the deviations in the diameter exponent p are quite large as expected. In fitting the coexistence curve one point near T_c, which was obviously inconsistent with the other data points was discarded. If this point is included in the least-square calculation a poorer fit is obtained and $\beta = 0.38$.

E. Triethylamine–Water [19]

The coexistence curve is unsymmetrical with respect to X_c as indicated in the deviation plot, figure 8. This asymmetry explains the low value of β in the fit $|X - X_c| = A|T - T_c|^\beta$ in the table II. Whereas the data are scattered near T_c, the diameter appears to curve when compositions are expressed in volume fraction and to a

greater extent in terms of mole fraction. It should be mentioned that Kohler and Rice were not able to decide whether the coexistence curve possessed a "flat top" from this data.

The apparent high value of β in table IV when compositions are expressed in mole fraction may well be a consequence of having only four experimental points on the right side of the coexistence curve. One point suggested to be in error by the authors was discarded in the analysis.

F. *n*-Decane–β-β'-Dichlorodiethylether [20]

The rather scattered data do not fit any of the equations to within the precision reported, and the adjusted value of T_c is 0.018 °C lower than the experimental value. The coexistence curve appears fairly symmetrical in terms of mole fraction, and the diameter is best represented by a straight line through the scattered points.

G. Water–Ethylene Glycol Monoisobutyl Ether [22]

Contrary to the conclusion in the original paper, the coexistence curve appears unsymmetrical as can be seen from the deviation plot, figure 11, for the fit $|X-X_c|=A|T-T_c|^\beta$, and this view is further supported by the low value of β in table II. Even though measurements were not made very close to T_c, the diameter possesses appreciable curvature as shown in figure 39 and table V.

H. Isobutyric Acid–Water [21]

For this system the adjusted value of T_c is 0.03 °C lower than the reported experimental value. The coexistence curve is very unsymmetrical with respect to X_c (see fig. 10 and table II) and the diameter is significantly curved as shown in figure 38.

I. Methyldiethylamine–Water [23]

In this less precise work the coexistence curve appears fairly symmetrical in terms of volume fraction, with the diameter best represented by a straight line. In terms of mole fraction (not reported here) the coexistence curve becomes very unsymmetrical and $\beta > 0.4$. Due to the low precision the behavior of the diameter cannot be deduced.

This work was supported in part by the Office of Standard Reference Data, National Bureau of Standards, under contract CST 761–5–69. We would like to thank Professor M. S. Green and Dr. F. Cook for helpful discussions. We are especially indebted to Dr. J. M. H. Levelt Sengers for advice, guidance, and finally very helpful criticism.

7. References

[1] T. Andrews, Phil. Mag., **4** (39), 150 (1870).
[2] J. D. van der Waals, Z. Physik. Chem. **13,** 657 (1894).
[3] J. M. H. Levelt Sengers, J. Straub, and M. Vicentini-Missoni, J. Chem. Phys. **54,** 5034 (1971).
[4] J. J. van Laar, Proc. Koninkl. Akad. Wetenschap. Amsterdam. **14,**[I] 428 (1911–1912); **14,**[II] 1091 (1911–1912).
[5] M. S. Green and J. V. Sengers, "Critical Phenomena, Proceedings of Conference," Nat. Bur. Stand. (U.S.), Misc. Publ. 273 (1966).
[6] E. A. Guggenheim, J. Chem. Phys. **13,** 253 (1945).
[7] B. H. Zimm, J. Chem. Phys. **20,** 538 (1952).
[8] O. K. Rice, Chem. Rev. **44,** 69 (1949); J. Chem. Phys. **15,** 314 (1917).
[9] J. D. Cox and E. F. G. Herington, Trans. Faraday Soc., **52,** 926 (1956).
[10] O. K. Rice, J. Phys. Colloid Chem. **54,** 1293 (1950); J. Chem. Phys. **23,** 164–8 (1955); ibid., **23,** 169 (1955).
[11] R. Thompson and O. K. Rice, J. Am. Chem. Soc. **86,** 3547 (1964).
[12] P. Heller, Rept. Progr. Phys. **30,** Part 2, 731 (1967).
[13] H. E. Stanley, "Introduction to Phase Transitions and Critical Phenomena," Oxford, 1971, p. 12.
[14] Ibid., p. 18.
[15] S. Michaels, M. S. Green, and S. Y. Larsen, "Equilibrium Critical Phenomena in Fluids and Mixtures," Nat. Bur. Stand. (U.S.) Misc. Publ. 327 (1970).
[16] A. M. Wims, D. McIntyre, and F. Hynne, J. Chem. Phys. **50,** 616 (1969).
[17] N. F. Irani and O. K. Rice, Trans. Faraday Soc. **63,** 2158 (1967).
[18] A. W. Loven and O. K. Rice, Trans. Faraday Soc. **59,** 2723 (1963).
[19] F. Kohler and O. K. Rice, J. Chem. Phys. **26,** 1614 (1957).
[20] B. Chu and W. P. Kao, J. Chem. Phys. **42,** 2608 (1965).
[21] D. Woermann and W. Sarholz, Ber. Bunsenges. Physik. Chem. **69,** 319 (1965).
[22] D. F. P. Rudd and B. Widom, J. Chem. Phys. **33,** 1816 (1960).
[23] J. L. Copp, Trans. Faraday Soc. **51,** 1056 (1955).
[24] W. E. Deming, "Statistical Adjustment of Data," Wiley, 1935.
[25] B. Widom and J. S. Rowlinson, J. Chem. Phys. **52,** 1670 (1970).
[26] N. D. Mermin, Phys. Rev. Letters **26,** 169 (1971).
[27] P. C. Hemmer and G. Stell, Phys. Rev. Letters **24,** 1284 (1970).
[28] M. S. Green, M. J. Cooper, and J. M. H. Levelt Sengers, Phys. Rev. Letters **26,** 492 (1971).
[29] M. E. Jacox, J. T. MacQueen, and O. K. Rice, J. Phys. Chem. **64,** 972 (1960).

Systems

A. Perfluoromethylcyclohexane–Carbon Tetrachloride, Thompson and Rice [11]

B. Nitroethane–3-Methylpentane, Wims, McIntyre, and Hynne [16]

C. Cyclohexane–Diiodomethane, Irani and Rice [17]

D. 2,6-Dimethylpyridine–Water, Loven and Rice [18]

E. Triethylamine–Water, Kohler and Rice [19]

F. *n*-Decane–β-β'-Dichlorodiethyl Ether, Kao and Chu [20]

G. Isobutyric Acid–Water, Woermann and Sarholz [21]

H. Ethylene Glycol Monoisobutyl Ether–Water, Rudd and Widom [22]

I. Methyldiethylamine–Water, Copp [23]

Tables

TABLE I. Description of systems

System	Type C.P.[a]	Composition variable	Experimental method	Number of points	Precision		Range in $\|\epsilon\|$
					Temperature (°C)	Concentration (%)	
A	U	Density	Mechanical Densitometer	14	0.00005	0.003	$2\times10^{-7}-1.9\times10^{-5}$
B	U	Density	Magnetic Densitometer	20	.001	.027	$2.3\times10^{-5}-1.0\times10^{-2}$
		Mole fraction nitroethane		20	.001	.5	
		Volume fraction nitroethane		20	.001	.5	
C	U	Mole fraction cyclohexane	Visual	14	.001	.21	$3.3\times15^{-5}-6.7\times10^{-3}$
D	L	Mole fraction pyridine	Visual	12	.001	.66	$6.8\times10^{-6}-4.0\times10^{-4}$
		Volume fraction pyridine		12	.001	.66	$6.8\times10^{-6}-4.0\times10^{-4}$
E	L	Mole fraction water	Visual	10	.001	.12	$2.1\times10^{-5}-4.4\times10^{-3}$
		Volume fraction water		10	.001	.75	$2.1\times10^{-5}-4.4\times10^{-3}$
F	U	Mole fraction *n*-decane	Visual	10	0.001, .01	.10	$1.3\times10^{-5}-1.3\times10^{-2}$
G	U	Mole fraction isobutyric acid	Visual	11	.01	.81	$1.0\times10^{-4}-8.2\times10^{-3}$
H	L	Mole fraction ether	Visual	16	.01	1.8	$1.3\times10^{-3}-2.5\times10^{-2}$
I	L	Mole fraction amine	Visual	11	.01	5.9	$3.1\times10^{-5}-1.4\times10^{-2}$

[a] Type of critical point: Upper (U) or Lower (L).

TABLE II. Coexistence curve fitted to $|X-X_c|=A|T-T_c|^{\beta}$

System	Composition variable	β	A	X_c	T_c (Fit)	T_c (Experimental)	Number of points	Reduced chi-square
A	Density	$0.356\pm.01$	$0.0260\pm.0006$	1.63415	28.6262	28.626	14	0.77
B	Density	$.324\pm.01$	$.0475\pm.0003$	0.7956	26.449	26.453	20	78.3
C	Mole fraction	$.342\pm.006$	$.1430\pm.0006$	.4120	28.564	28.564	14	6.0
D	Mole fraction	$.341\pm.04$	$.0396\pm.001$	.0645	33.929	33.927	12	1.8
E	Mole fraction	$.175\pm.04$	$.0635\pm.003$	.907	18.330	18.33	10	4.8
F	Mole fraction	$.325\pm.01$	$.1426\pm.0005$	.399	26.480	26.50	10	69.1
G	Mole fraction	$.232\pm.02$	$.0474\pm.0005$	.120	26.25	26.30	11	12.5
H	Mole fraction	$.168\pm.03$	$.0418\pm.001$	.0794	25.80	25.8	16	23.7
I	Volume fraction	$.293\pm.03$	$.202\pm.005$	.43	49.42	49.42	11	0.81

TABLE III. Coexistence curve fitted to: $(X^+ - X_c) = A^+ |T - T_c|^{\beta+}, X^+ > X_c$
$(X_c - X^-) = A^- |T - T_c|^{\beta-}, X_c > X^-$

System	Composition variable	β^+	β^-	A^+	A^-	T_c	X_c	Number of points		$R\chi^2$
								+	−	
A	Density.....	0.283 ± .01	0.379 ± .01	0.0206 ± .001	0.0255 ± .002	28.62601	1.63470	7	7	0.25
B	Density.....	.279 ± .004	.385 ± .002	.0482 ± .0001	.0465 ± .0001	26.452	0.7970	10	10	3.16
B	Mole fraction.....	.352 ± .005	.303 ± .007	.138 ± .001	.135 ± .001	26.454	.497	10	10	0.44
B	Volume fraction.....	.312 ± .004	.343 ± .006	.1213 ± .0005	.1298 ± .001	26.453	.358	10	10	0.53
C	Mole fraction.....	.328 ± .010	.359 ± .006	.144 ± .003	.141 ± .001	28.564	.414	6	8	6.47
D	Mole fraction.....	.329 ± .020	.393 ± .026	.0359 ± .002	.0478 ± .004	33.928	.0640	6	6	0.99
D	Volume fraction.....	.356 ± .03	.365 ± .03	.1436 ± .009	.1504 ± .010	33.928	.3060	6	6	0.94
E	Mole fraction.....	.477 ± .05	.185 ± .01	.119 ± .007	.058 ± .001	18.329	.915	7	4	3.10
E	Volume fraction.....	.354 ± .02	.252 ± .02	.276 ± .008	.225 ± .006	18.329	.600	7	4	2.7
F	Mole fraction.....	.297 ± .011	.346 ± .016	.1409 ± .001	.1408 ± .001	26.480	.399	5	5	39.40
G	Mole fraction.....	.258 ± .020	.482 ± .026	.0444 ± .0004	.0606 ± .0007	26.29	.118	6	5	3.10
H	Mole fraction.....	.172 ± .01	.474 ± .02	.0356 ± .0003	.0344 ± .0006	25.85	.0720	8	8	0.54
I	Volume fraction.....	.29 ± .03	.35 ± .06	.174 ± .005	.229 ± .008	49.42	.40	6	5	0.33

TABLE IV. Coexistence curve fitted to $X^+ - X^- = A |\epsilon|^\beta, X^+ > X^-$

System	Composition variable	β	A	T_c (Fit)	T_c (Experimental)	Reduced chi-square
A	Density.....	0.333 ± .018	0.313 ± .05	28.62606	28.626	0.37
B	Density.....	.333 ± .004	0.633 ± 0.21	26.455	26.453	1.48
	Volume fraction.....	.332 ± .007	1.66 ± .042	26.455	26.453	0.19
	Mole fraction.....	.332 ± .007	1.814 ± .052	26.455	26.453	0.24
C	Mole fraction.....	.342 ± .004	2.015 ± .025	28.564	28.564	2.09
D	Volume fraction.....	.339 ± .041	1.951 ± .70	33.929	33.927	0.11
	Mole fraction.....	.340 ± .037	0.556 ± .20	33.929	33.927	0.14
E	Volume fraction.....	.332 ± .033	3.421 ± .27	18.325	18.33	1.13
	Mole fraction.....	.372 ± .037	1.467 ± .70	18.324	18.33	2.32
F	Mole fraction.....	.324 ± .009	1.778 ± .013	26.482	26.50	11.4
G	Mole fraction.....	.335 ± .029	0.695 ± .10	26.27	26.30	1.48
H	Mole fraction.....	.345 ± .021	0.4948 ± .041	25.81	25.8	0.10
I	Volume fraction.....	.336 ± .03	2.767 ± .21	49.42	49.42	0.15

TABLE V. Diameter fitted to $\bar{X}/X_c = 1 + a|\epsilon|^p$

System	Composition variable	X_c	a	p	$R\chi^2$
A	Density			$< \beta^c$	
B[a]	Density	0.7936 ± .0003	0.39 ± .01	0.85 ± .06	2.30
		.7931 ± .0008	0.115 ± .04	0.53 ± .21	16.26
B	Mole fraction	.501 ± .001	− 0.50 ± .06	0.67 ± .20	0.39
		.501 ± .001	− 2.12 ± .7	0.95 ± .42	5.77
B Run A	Volume fraction	.357 ± .001	0.58 ± .07	0.62 ± .21	0.31
Run B				$< \beta^c$	
C[b]	Mole fraction	.4111 ± .0005	1.19 ± 3	1.0 ± .5	2.65
D	Volume fraction	.3062 ± .002	3.85 ± 180	0.97 ± 1	0.04
D	Mole fraction	.0636 ± .002	3.61 ± 31	0.62 ± .13	0.56
E	Volume fraction	.609 ± .001	− 5.12 ± .44	0.75 ± .04	1.77
E	Mole fraction	.9242 ± .0008	− 1.31 ± .08	0.60 ± .03	2.86
F	Mole fraction	.3953 ± .0016	2.38 ± 3.7	1.0 ± .4	17.20
G	Mole fraction	.1127 ± .002	1.77 ± .8	0.49 ± .11	0.18
H	Mole fraction	.0624 ± .002	4.10 ± 1.4	0.59 ± .11	0.09
I	Volume fraction	.41 ± .005	8.54 ± 6.8	1.0 ± 1	0.02

[a] Both coexisting composition variables experimentally available at each temperature.
[b] Coexisting composition variable obtained by interpolation.
[c] The value of the parameter β was lower than the lowest value in the grid searching procedure.

Figures

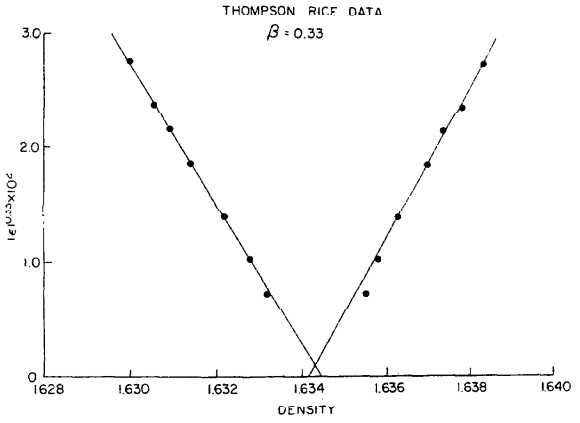

FIGURE 1. Cox-Herrington plot for the system perfluoromethylcyclohexane–carbon tetrachloride [11] using $\beta = 0.33$.

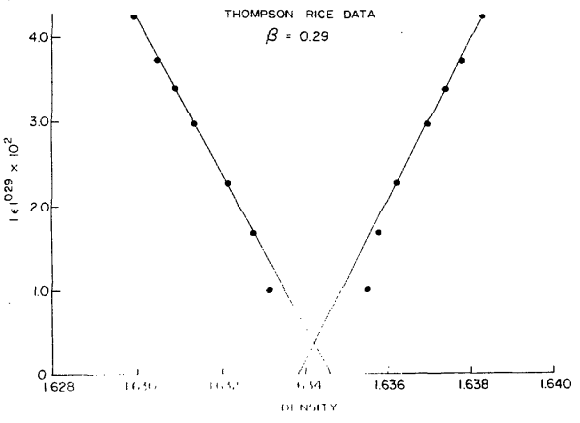

FIGURE 2. Cox-Herrington plot for the system perfluoromethylcyclohexane–carbon tetrachloride [11] using $\beta = 0.29$.

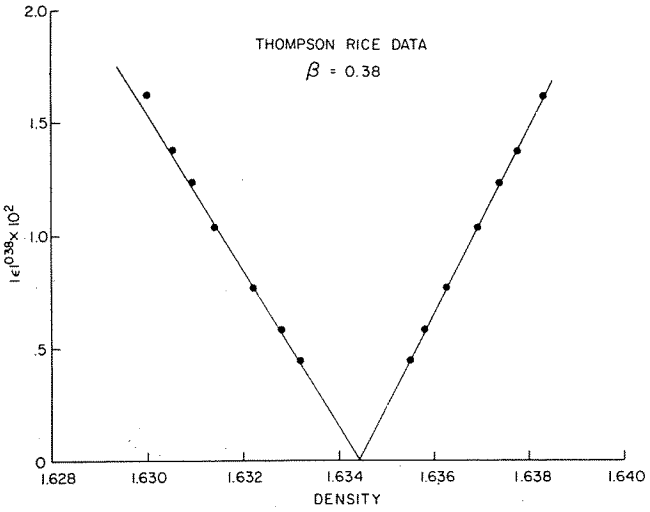

FIGURE 3. Cox-Herrington plot for the system perfluoromethylcyclohexane–carbon tetrachloride [11] using $\beta = 0.38$.

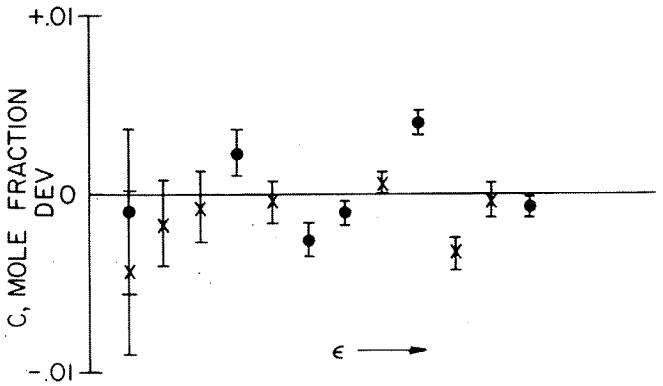

FIGURE 6. Coexistence curve deviation plots resulting from fitting the data to $|X - X_c| = A\,\epsilon^{\beta}$ for the systems: cyclohexane–*d*-iodomethane [17]. x left branch, · right branch.

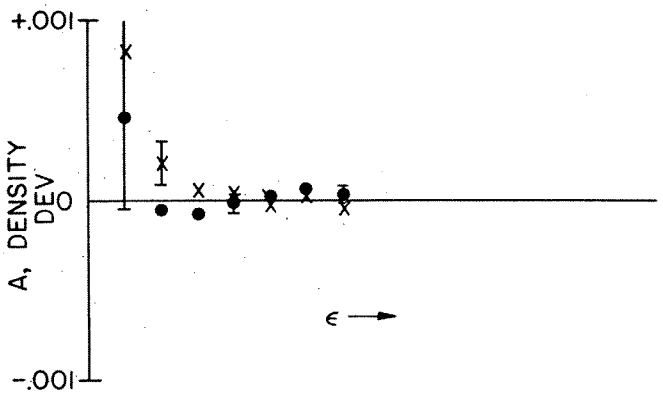

FIGURE 4. Coexistence curve deviation plots resulting from fitting the data to $|X - X_c| = A\,\epsilon^{\beta}$ for the systems: perfluoromethylcyclohexane–carbon tetrachloride [11]. x left branch, · right branch.

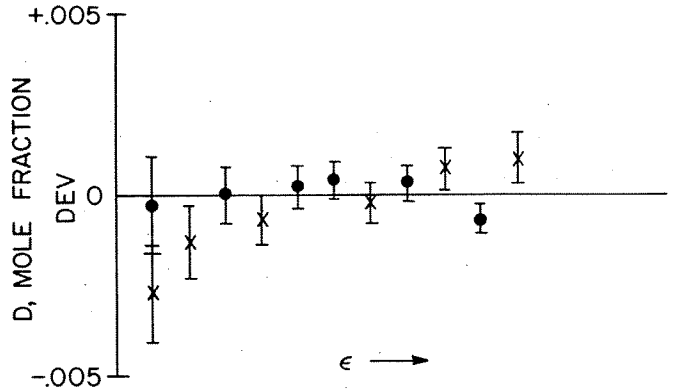

FIGURE 7. Coexistence curve deviation plots resulting from fitting the data to $|X - X_c| = A\,\epsilon^{\beta}$ for the systems: 2,6-dimethylpyridine–water [18]. x left branch, · right branch.

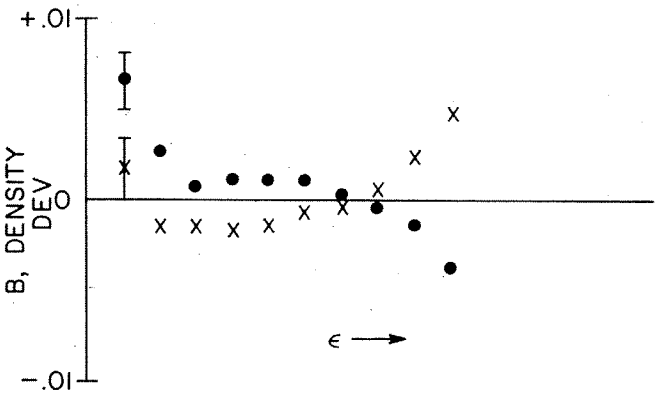

FIGURE 5. Coexistence curve deviation plots resulting from fitting the data to $|X - X_c| - A\,\epsilon^{\beta}$ for the systems: nitroethane–3-methylpentane [16]. x left branch, right branch.

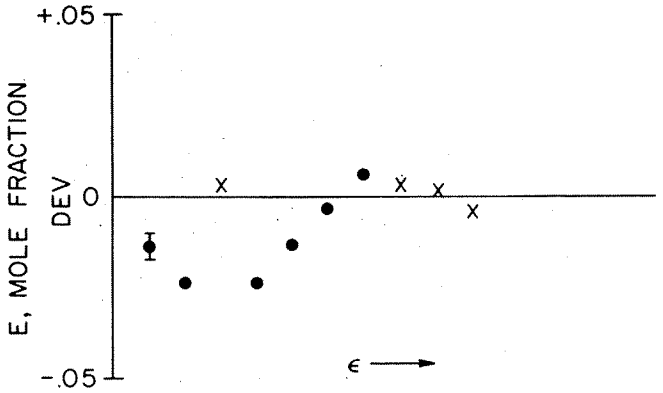

FIGURE 8. Coexistence curve deviation plots resulting from fitting the data to $|X - X_c| = A\,\epsilon^{\beta}$ for the systems: triethylamine–water [19]. x left branch, · right branch.

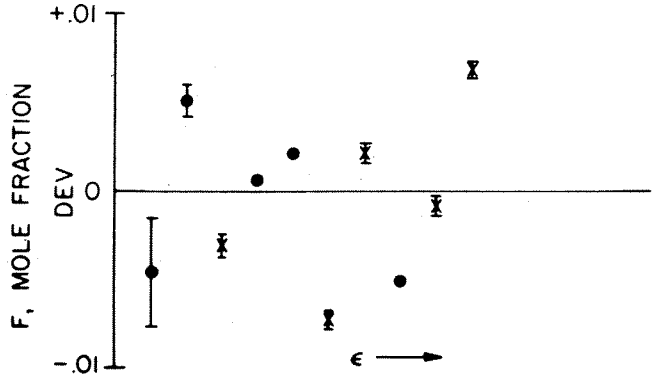

FIGURE 9. Coexistence curve deviation plots resulting from fitting the data to $|X-X_c|=A\,\epsilon^{\beta}$ for the systems: η-decane–β-β'-dichlorodiethylether [20]. x left branch, · right branch.

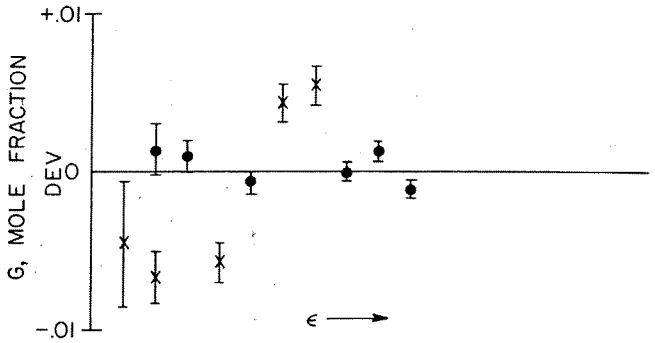

FIGURE 10. Coexistence curve deviation plots resulting from fitting the data to $|X-X_c|=A\,\epsilon^{\beta}$ for the systems: isobutyric acid–water [21]. x left branch, · right branch.

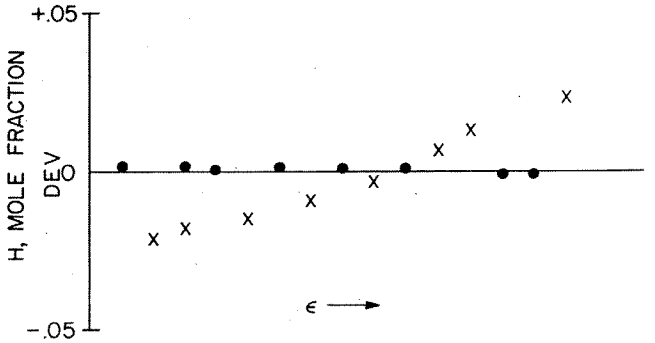

FIGURE 11. Coexistence curve deviation plots resulting from fitting the data to $|X-X_c|=A\,\epsilon^{\beta}$ for the systems: water–ethylene glycol monoisobutyl ether [22]. x left branch, · right branch.

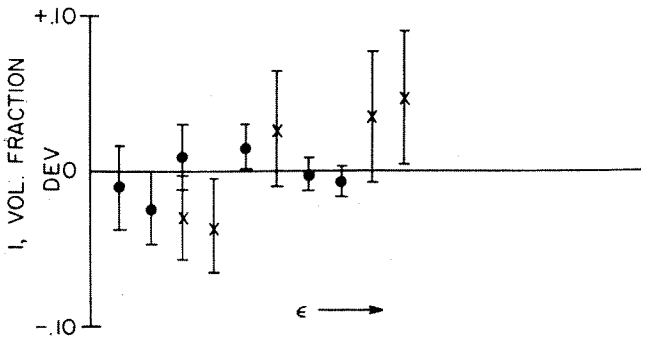

FIGURE 12. Coexistence curve deviation plots resulting from fitting the data to $|X-X_c|=A\,\epsilon^{\beta}$ for the systems: methyldiethylamine–water [23]. x left branch, · right branch.

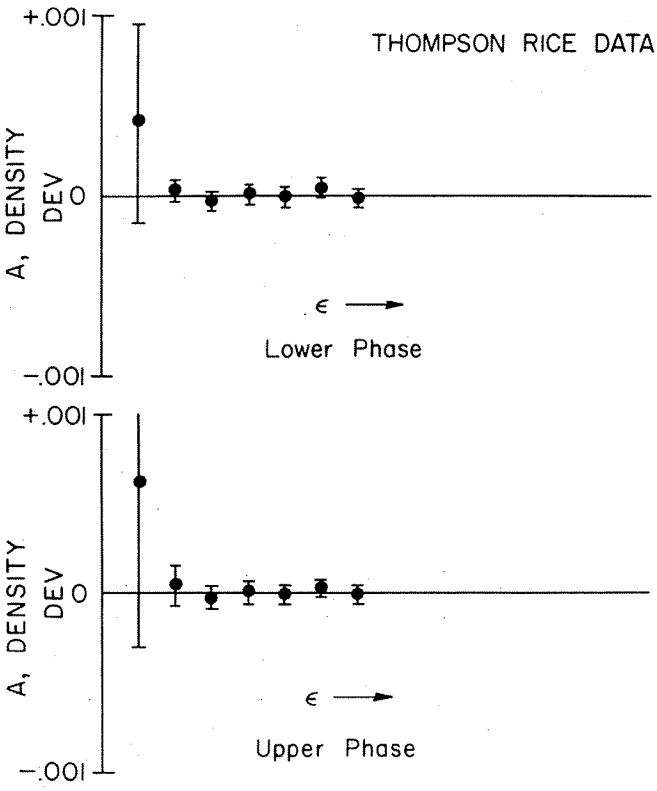

FIGURE 13. Coexistence curve deviation plots resulting from fitting each side of the coexistence curve separately to the equations $X^{-}=A^{-}+B^{-}|T-C^{-}|^{d-}$; $X_c>X^{-}$ (upper plot) and $X^{+}=A^{+}+B^{+}|T-C^{+}|^{d+}$; $X^{+}>X_c$ (lower plot) for the system perfluoromethylcyclohexane–carbon tetrachloride [11].

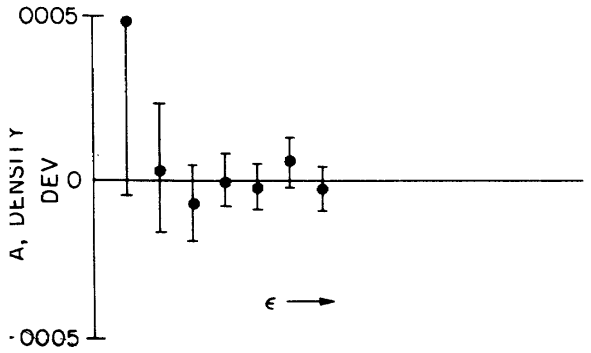

FIGURE 14. Coexistence curve deviation plot resulting from fitting the data to $X^+ - X^- = A|\epsilon|^\beta$; $X^+ > X^-$ for the system perfluoromethylcyclohexane – carbon tetrachloride [11].

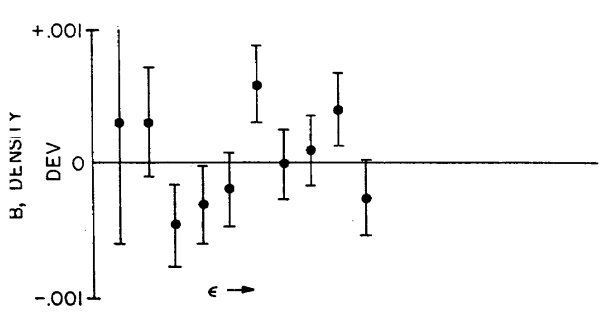

FIGURE 15. Coexistence curve deviation plots resulting from fitting the data to $X^+ - X^- = A|\epsilon|^\beta$, for the system nitroethane–3-methylpentane [16]. Order parameter X as density.

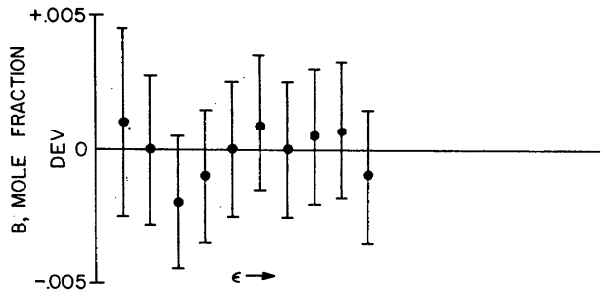

FIGURE 16. Coexistence curve deviation plots resulting from fitting the data to $X^+ - X^- = A|\epsilon|^\beta$ for the system nitroethane–3-methylpentane [16]. Order parameter X as mole fraction.

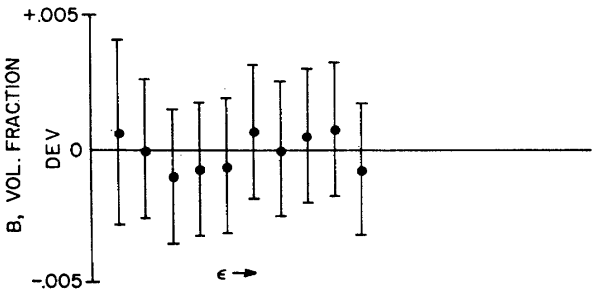

FIGURE 17. Coexistence curve deviation plots resulting from fitting the data to $X^+ - X^- = A|\epsilon|^\beta$ for the system nitroethane–3-methylpentane [16]. Order parameter X as volume fraction.

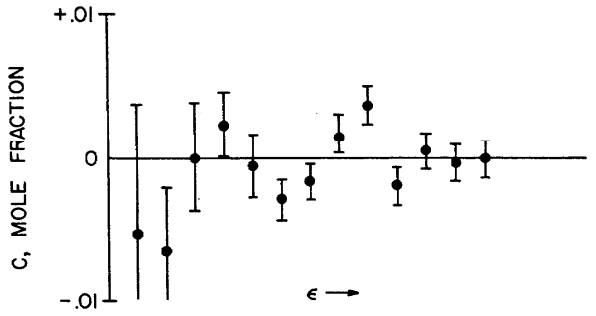

FIGURE 18. Coexistence curve deviation plots resulting from fitting the data to $X^+ - X^- = A|\epsilon|^\beta$ using one data point and one smoothed point as discussed in the text for the systems: cyclohexane–diiodomethane [17].

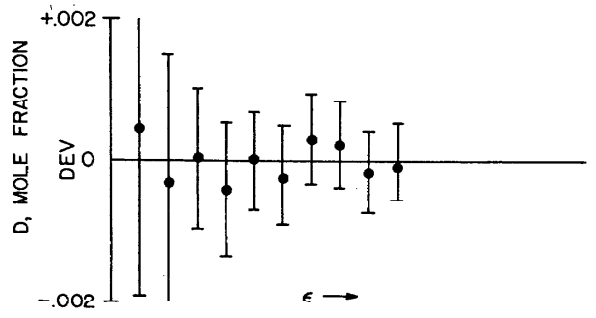

FIGURE 19. Coexistence curve deviation plots resulting from fitting the data to $X^+ - X^- = A|\epsilon|^\beta$ using one data point and one smoothed point as discussed in the text, for the systems: 2,6-dimethylpyridine – water [18], X as mole fraction.

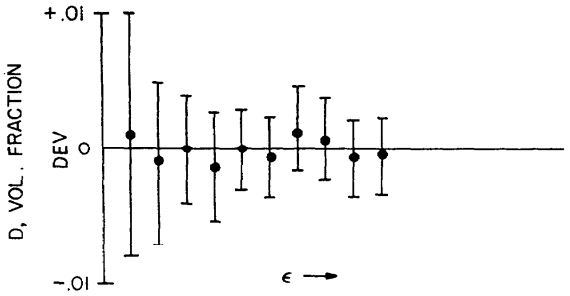

FIGURE 20. Coexistence curve deviation plots resulting from fitting the data to $X^+ - X^- = A|\epsilon|^\beta$ using one data point and one smoothed point as discussed in the text, for the systems: 2.6-dimethylpyridine–water [18], X as volume fraction.

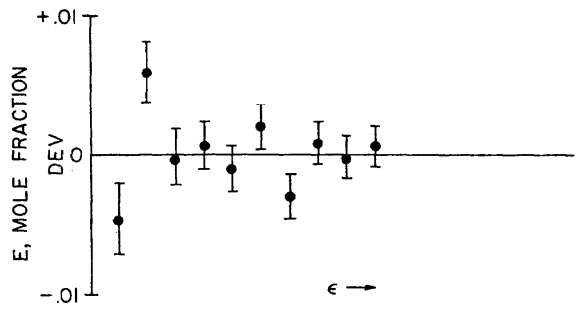

FIGURE 21. Coexistence curve deviation plots resulting from fitting the data to eq (24) as described in the text for the systems: triethylamine–water [19]. X as mole fraction.

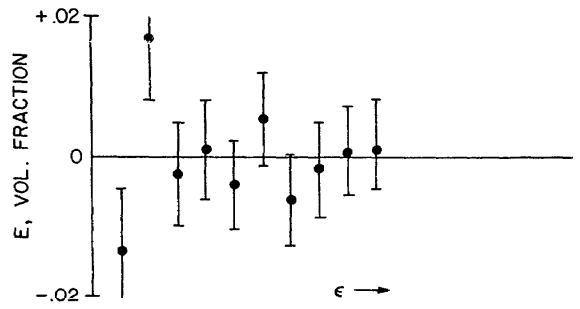

FIGURE 22. Coexistence curve deviation plots resulting from fitting the data to eq (24) as described in the text for the systems: triethylamine–water [19] X as volume fraction.

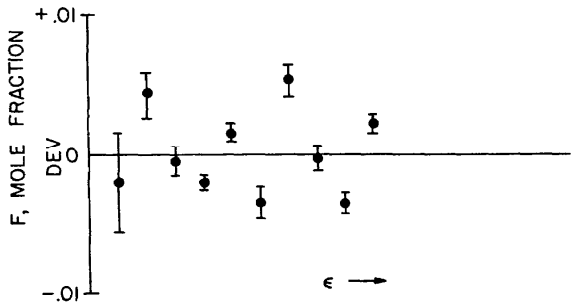

FIGURE 23. Coexistence curve deviation plots resulting from fitting the data to eq (24) as described in the text for the systems: η-decane–β-β'-dichloro diethylether [20].

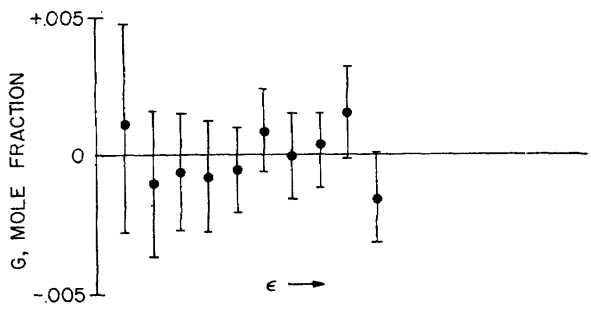

FIGURE 24. Coexistence curve deviation plots resulting from fitting the data to eq (24) as described in the text for the systems: isobutyric acid–water [21].

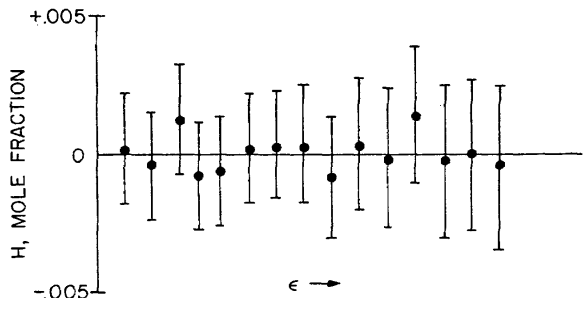

FIGURE 25. Coexistence curve deviation plots resulting from fitting the data to eq (24) as described in the text for the systems: water–ethylene glycol monoisobutyl ether [22].

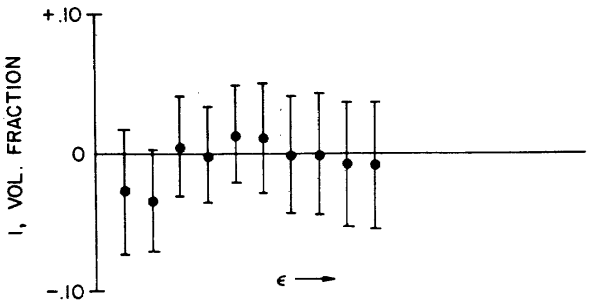

FIGURE 26. Coexistence curve deviation plots resulting from fitting the data to eq (24) as described in the text for the systems: methyldiethylamine–water [23].

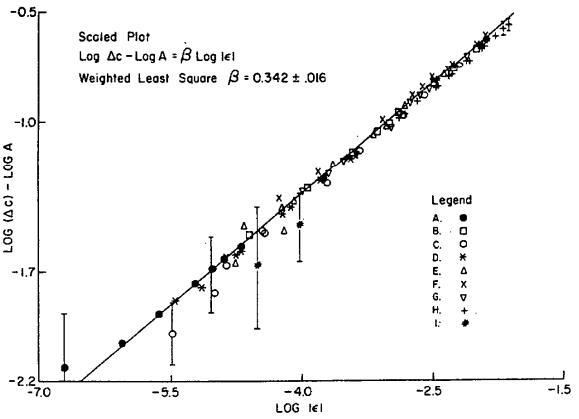

FIGURE 27. Scaled plot for all systems. The data were fit to the equation $\log \Delta_c - \log A = \beta \log |\epsilon|$. Composition variables correspond to table 2.

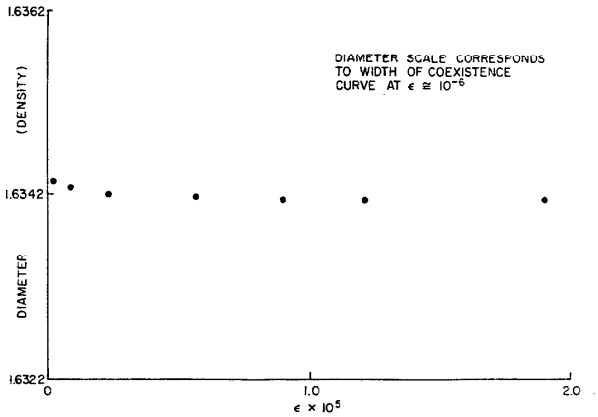

FIGURE 28. Diameter $(X^+ + X^-)/2$ as a function of the reduced temperature $(T - T_c)/T_c$ perfluoromethylcyclohexane–carbon tetrachloride [11].

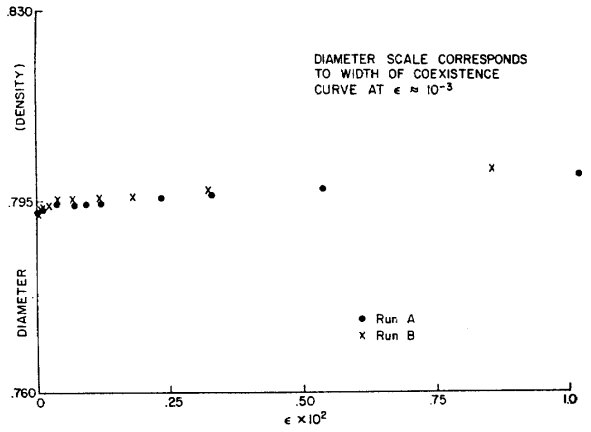

FIGURE 29. Diameter as a function of reduced temperature for the system nitroethane–3-methylpentane. The order parameter, X, is taken as density.

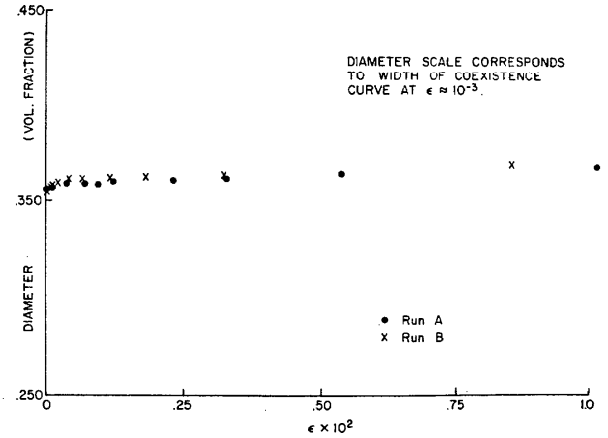

FIGURE 30. Diameter as a function of reduced temperature for the system nitroethane–3-methylpentane. The order parameter, X, is taken as a volume fraction.

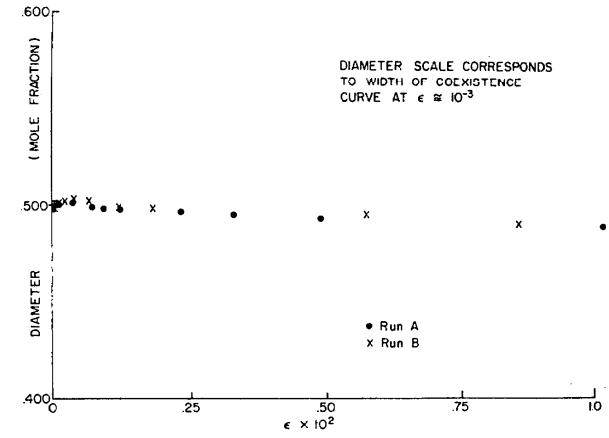

FIGURE 31. Diameter as a function of reduced temperature for the system nitroethane–3-methylpentane. The order parameter, X, is taken as mole fraction.

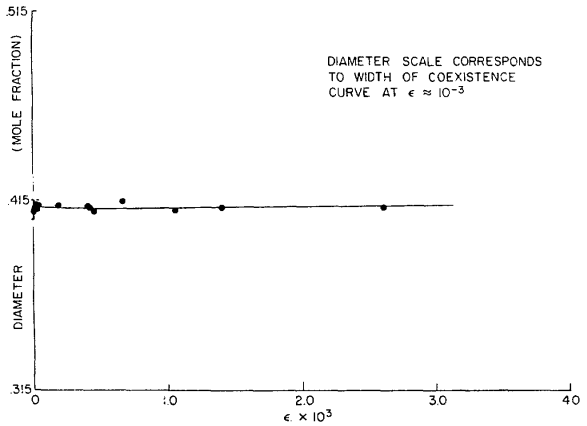

FIGURE 32. Diameter as a function of reduced temperature for the system cyclohexane–diiodomethane. The solid line indicates the least squares curve.

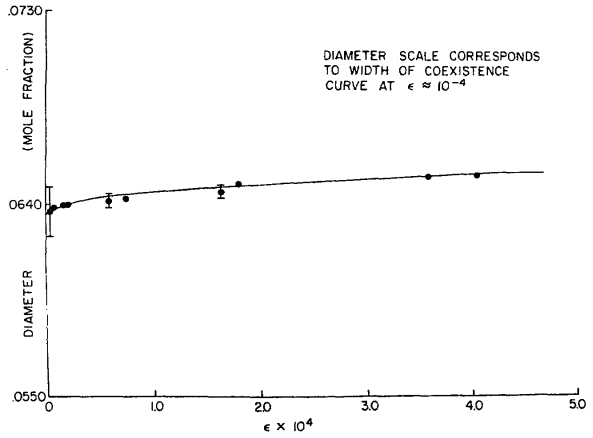

FIGURE 33. Diameter versus reduced temperature for the system 2,6-dimethylpyridine–water. The order parameter, X, is taken as mole fraction. The solid line indicates the least squares curve.

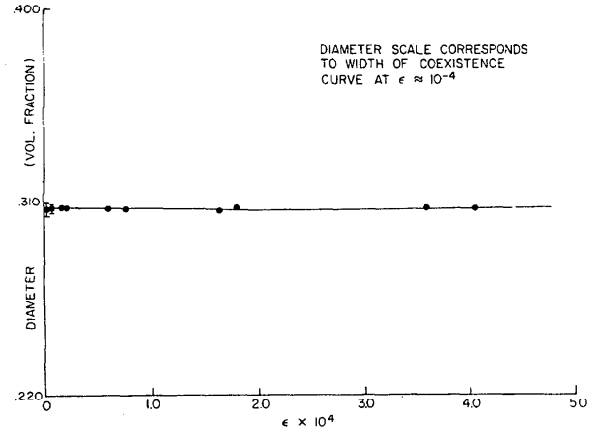

FIGURE 34. Diameter versus reduced temperature for the system 2,6-dimethylpyridine–water. The order parameter, X, is taken as volume fraction. The solid line indicates the least squares fitted curve.

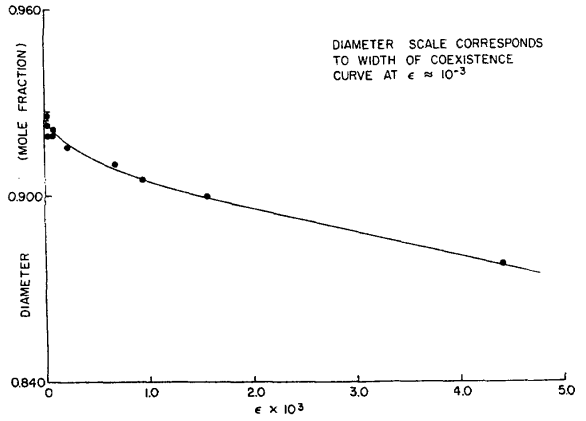

FIGURE 35. Diameter versus reduced temperature for the system triethylamine–water. The order parameter, X, is taken as mole fraction. The solid line indicates the least squares fitted curve.

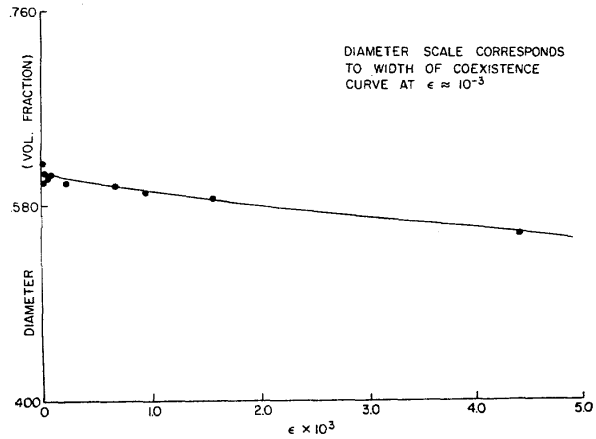

FIGURE 36. Diameter versus reduced temperature for the system triethylamine–water. The order parameter, X, is taken as volume fraction. The solid line indicates the least square fitted curve.

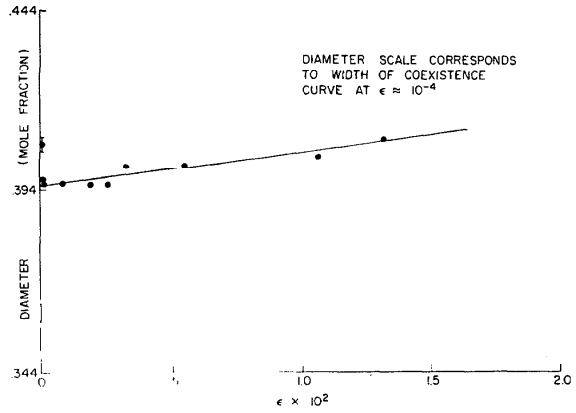

FIGURE 37. Diameter versus reduced temperature for the system η-decane–β-β'-dichlorodiethylether. The solid line indicates the least squares fitted curve.

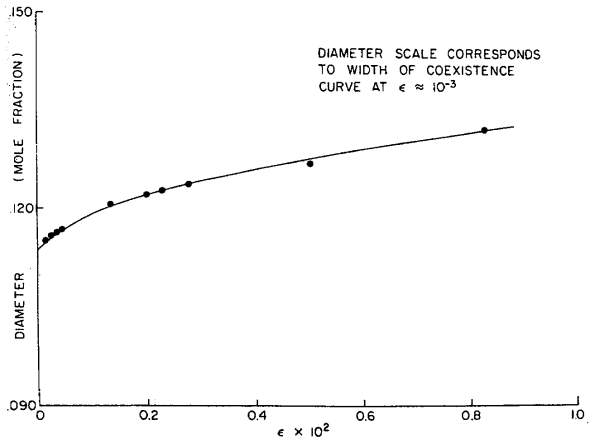

FIGURE 38. Diameter versus reduced temperature for the system isobutyric acid–water. The solid line indicates the least squares fitted curve.

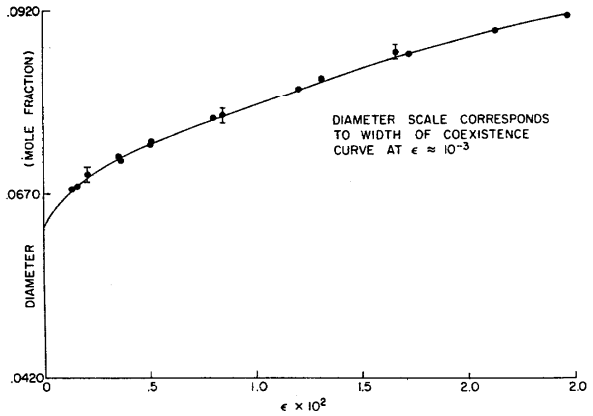

FIGURE 39. Diameter versus reduced temperature for the system ethylene glycol monoisobutyl ether–water. The solid line represents the least squares fitted curve.

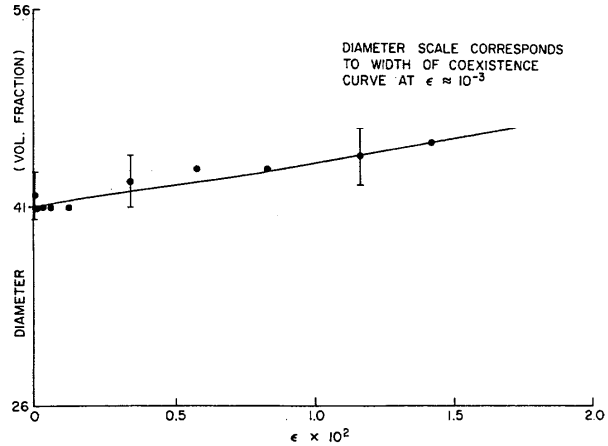

FIGURE 40. Diameter versus reduced temperature for the system methyldiethylamine–water. The solid line indicates the least squares fitted curve.

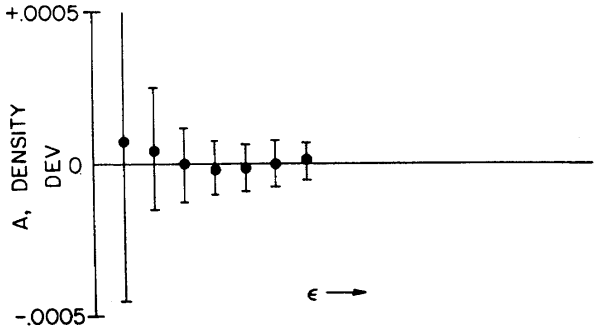

FIGURE 41. Diameter deviation plots resulting from fitting the data to eq (34) for the systems: perfluoromethylcyclohexane–carbon tetrachloride.

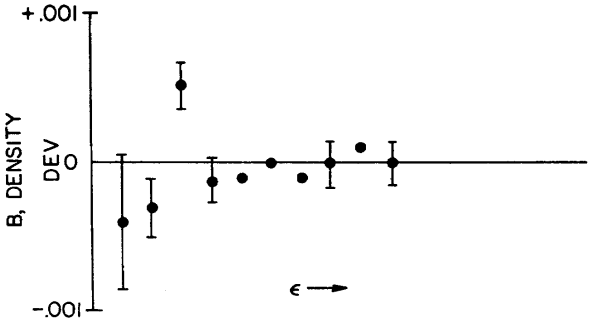

FIGURE 42. Diameter deviation plots resulting from fitting the data to eq (34) for the systems: nitroethane–3-methylpentane, the order parameter, X, taken as density.

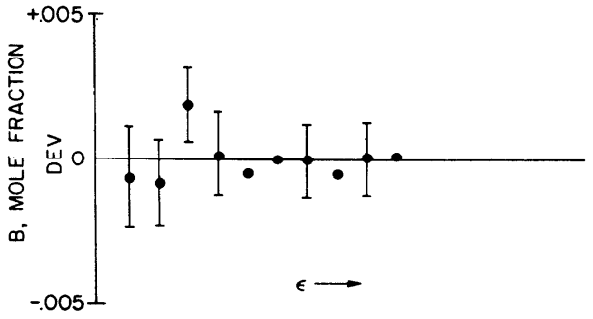

FIGURE 43. Diameter deviation plots resulting from fitting the data to eq (34) for the systems: nitroethane–3-methylpentane, the order parameter, X, taken as mole fraction.

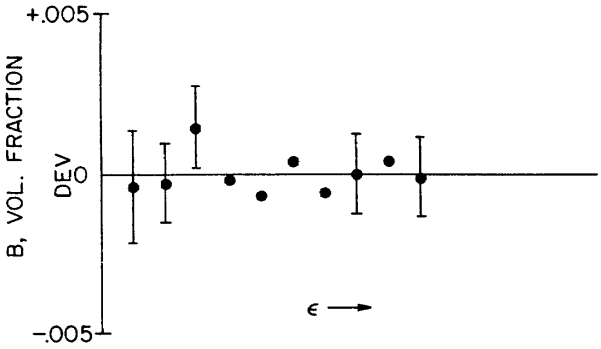

FIGURE 44. Diameter deviation plots resulting from fitting the data to eq (34) for the systems: nitroethane–3-methylpentane, the order parameter, X, taken as volume fraction.

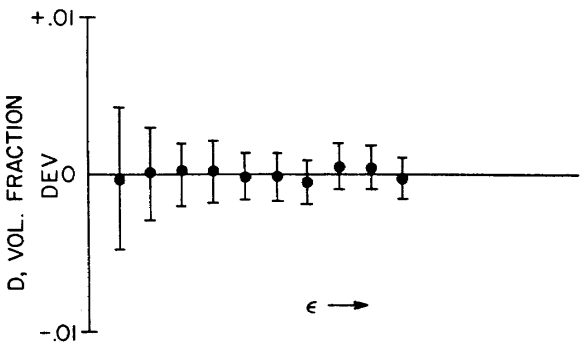

FIGURE 47. Diameter deviation plots resulting from fitting the data to eq (34) for the systems: 2,6-dimenthylpyridine–water, the order parameter, X, is taken as volume fraction.

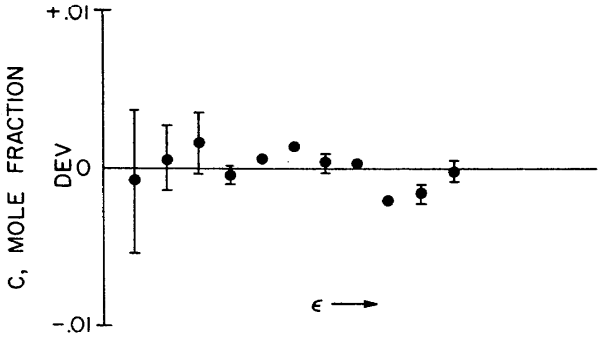

FIGURE 45. Diameter deviation plots resulting from fitting the data to eq (34) for the systems: cyclohexane–diiodomethane.

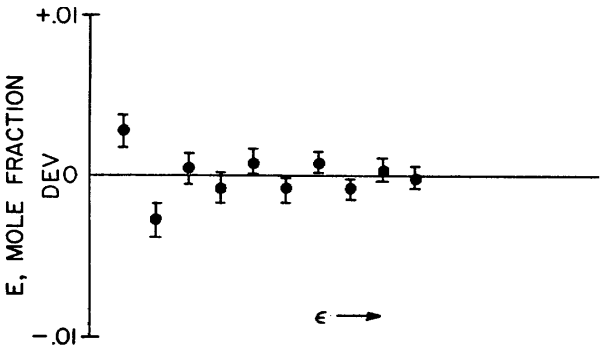

FIGURE 48. Diameter deviation plots resulting from fitting the data to eq (34) for the systems: triethylamine–water, the order parameter, X, is taken as mole fraction.

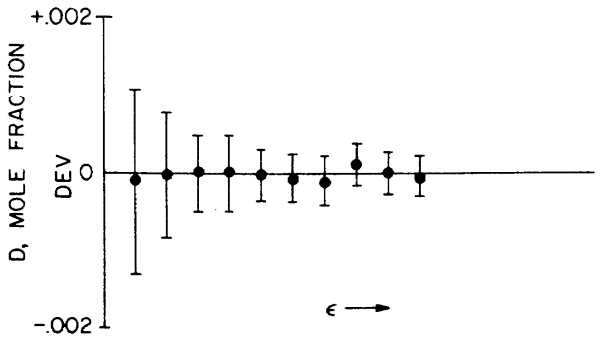

FIGURE 46. Diameter deviation plots resulting from fitting the data to eq (34) for the systems: 2,6-dimethylpyridine–water, the order parameter, X, taken as mole fraction.

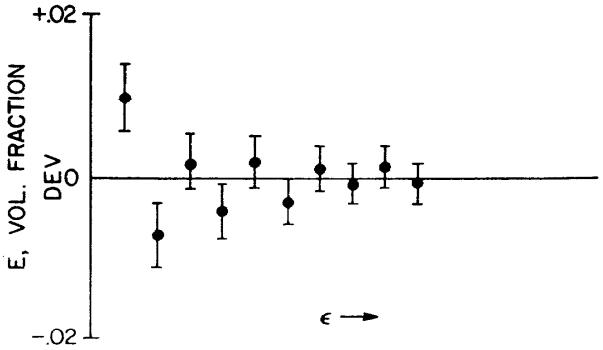

FIGURE 49. Diameter deviation plots resulting from fitting the data to eq (34) for the systems: triethylamine–water, the order parameter, X, is taken as volume fraction.

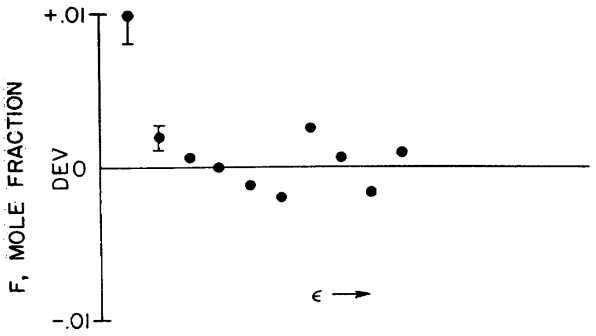

FIGURE 50. Diameter deviation plots resulting from fitting the data to eq (34) for the systems: η-decane–β-β'-dichlorodiethylether.

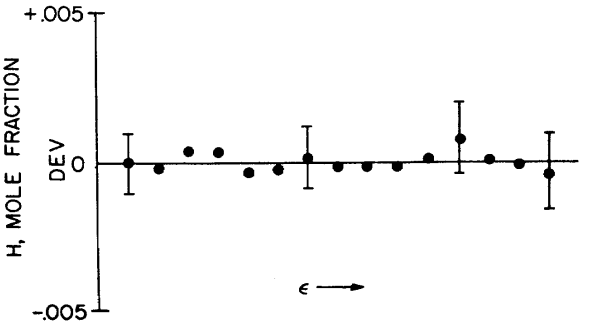

FIGURE 52. Diameter deviation plots resulting from fitting the data to eq (34) for the systems: water–ethylene glycol monoisobutyl ether.

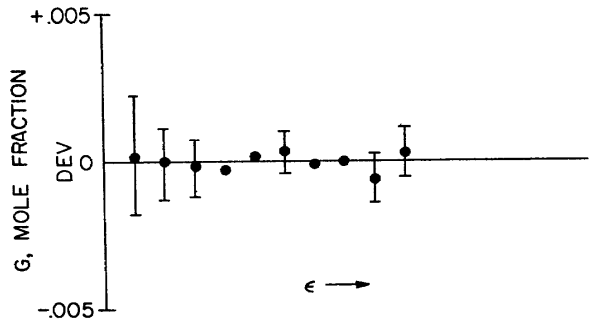

FIGURE 51. Diameter deviation plots resulting from fitting the data to eq (34) for the systems: isobutyric acid–water.

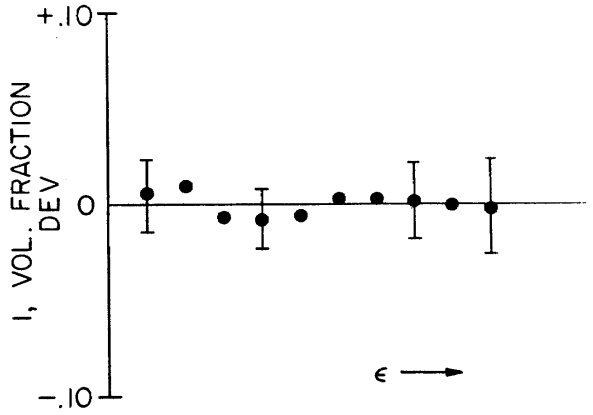

FIGURE 53. Diameter deviation plot resulting from fitting the data to eq (34) for the system methyldiethylamine–water.